Master Thesis
TVVR 22/5014

Groundwater Modelling in southeast Cambodia

Facing irrigation and groundwater changes during a pandemic

Svea Bertolatus

Division of Water Resources Engineering
Department of Building and Environmental Technology
Lund University

Groundwater Modelling in southeast Cambodia

Facing irrigation and groundwater level changes during a pandemic

By:
Svea Bertolatus

Master Thesis

Division of Water Resources Engineering
Department of Building & Environmental Technology
Lund University
Box 118
221 00 Lund, Sweden

Water Resources Engineering
TVVR-22/5014
ISSN 1101-9824

Lund 2022
www.tvrl.lth.se

Master Thesis
Division of Water Resources Engineering
Department of Building & Environmental Technology
Lund University

English title:	Groundwater Modelling in southeast Cambodia
Author(s):	Svea Bertolatus
Supervisor:	Hossein Hashemi Paul Pavelic
Examiner:	Ronny Berndtsson
Language	English
Year:	2022
Keywords:	Groundwater, modelling, irrigation, Cambodia, pandemic

Acknowledgments

I would like to express my sincere appreciation and gratitude to my two supervisors, Hossein Hashemi from Lund University and Paul Pavelic from IWMI Southeast Asia. Hossein has been my supervisor during the Bachelor thesis and has now again been supporting me with knowledge, patience, and motivation during this project and Master thesis work. I am very thankful for his support. Paul trusted me to take part in his research in Cambodia, gave me the opportunity to do the field study, and helped with guidance when I found myself in a challenging situation. I am grateful for his encouragement and knowledge during the past ten months. Further, I would like to give special thanks to my examiner, Ronny Berndtsson, for his flexibility and patience.

Furthermore, I want to thank Behshid Khodaei for her support and guidance in the remote sensing analysis, it was so helpful to discuss the methodology and learn from her experience with remote sensing. I also would like to express my appreciation to Mohammad Attari for helping me with Python coding in Google Earth Engine. I would further like to express appreciation to Gerhard Barmen, for trusting me by lending the University`s device, though it included challenges.

Furthermore, I would like to gratefully acknowledge the team at ITC in Phnom Penh for receiving and welcoming me in Cambodia with generosity and hospitality. Without you, it would have been impossible to carry out this field study. Therefore, I want to express special thanks to the advisor Sok Ty, and the students Chanseyma Khoeun, Penglong Koun and Attitya Mom for accompanying me to the provinces Prey Veng and Svay Rieng, helping with data collection and showing me culture and food. Maybe one day I will get the chance to welcome you in Sweden/ Germany as well. I would like to give a special thanks to Mathieu Viossanges for the immediate help in a challenging situation as well as the support with available data. Further, I want to thank Michael Roberts and Heng Bunthoeun for generously providing relevant data. I would like to say thank you to all other amazing friends and connections that I made during the stay and along the way, who are another reason for an incredibly amazing time. Thanks to the Crafoord Foundation for their support and giving me this opportunity.

Lastly, I want to thank my close friends and my family for their immense support in everyday life and challenging situations. Because of you I wake up happy every day and I am so extremely lucky and grateful to have you in my life.

Abstract
All countries in the Mekong region are dealing with the challenge of sustainable water resources management. In Cambodia, where rice production is of high importance for household food security and for export, groundwater is being used for irrigation during the dry season, since it has resulted in higher rice production. However, groundwater use is not regulated and often unplanned, thus, it is expected to cause the decline of the groundwater level in the region. Due to economic and challenges and restrictions during the pandemic, the irrigation pattern was expected to have changed.
To investigate the impact of changing irrigation patterns on groundwater levels during the pandemic a groundwater model using GMS MODFLOW was established, initially creating a steady-state model and then transitioning to a transient-state model, where evapotranspiration (ET) should be used as an indicator of groundwater irrigation. Established steady-state and transient state groundwater models were highly sensitive to recharge changes, and calibration led to acceptable error estimates. Calibrating the transient model showed surprisingly good results, considering that this part of Cambodia experiences dry and wet season and the steady state model was only done for a specific time in the dry season in 2006. The automated parameter estimation (PEST) faced computational issues. The analysis of groundwater levels showed an increased decline for the pandemic years compared to earlier years. The model was highly simplified due to data limitations, for instance regarding bedrock elevations and recharge parameters. Time regarding and spatial interpolations were done in order to receive continuous spatial datasets. Literature studies showed different ranges for certain parameter values. Larger geophysical investigations in the study area would add certainty and reliable input data, thus, improve the groundwater model. Other useful extensions are suggested to be added to GMS MODFLOW, for instance to add detail to the relationship of hydraulic head and ET.

Contents

List of Abbreviations

ET	Evapotranspiration
ETS	Evapotranspiration Segments
NDVI	Normalized Difference Vegetation Index
GEE	Google Earth Engine
IDE	International Development Enterprises
ITC	Institute of Technology of Cambodia
IWMI	International Water Management Institute
K	Hydraulic conductivity
ME	Mean Error
MAE	Mean Absolute Error
NGO	Non-governmental organisation
PEST	Parameter ESTimation
PDoWRAM	Provincial Departments of Water Resources and Meteorology
PRASAC	Programme de Réhabilitation et d'Appui au Secteur Agricole du Cambodge
USGS	United States Geological Survey
RMSE	Root Mean Square Error
T	Transmissivity

List of Tables

List of Figures

1. Introduction

The Mekong River is a transboundary river in East and Southeast Asia, having its source at the Tibetan Plateau in China, then passing through Myanmar, Lao PDR, Thailand, Cambodia and finally reaching the sea in Vietnam, via the Mekong Delta (Misachi, 2021). Sustainable water resources management is a challenge that all countries in the Mekong region are dealing with. Groundwater is of high importance, when surface water does not fulfil the needs in arid countries, and can also be relevant for water rich countries, when the surface water infrastructure is not sufficient. The benefit of groundwater usage is its private accessibility with infrastructure like dug wells or tube wells and suction pumps (Open Development, 2016). In the Lower Mekong region, groundwater starts playing a more and more important role for irrigation, industry, and households. Population is increasing and the economy is growing, which results in increased groundwater pumping for irrigation of farmland, while groundwater has also been used for domestic purposes for a long time. At the same time there is a global lack of information on groundwater resources and availability for sustainable usage (Open Development, 2016).

Looking at Cambodia, rice production is of high importance for household food security and for export. Especially in the dry season, the capacity for irrigation is low, and one fundamental factor limiting agricultural production (Erban and Gorelick, 2016). Compared to Vietnam (60 %), Cambodia's irrigation capacity lays far behind (10 %) (Erban and Gorelick, 2016). This is one reason why Vietnam is exporting six times more rice than Cambodia does. Nowadays, the planned upgrades of infrastructure to increase the access to surface water (45 % area increase of dry season crop, over the next 20 years) are being outpaced by the installation of motorized pump irrigation wells (20 % more installations per year). Analyses of landcover changes show that the amount of irrigated land increases at the same pace (20 % per year) (Erban and Gorelick, 2016). Using groundwater for irrigation has resulted in higher rice production and the ability to switch crops, however, the groundwater use is not regulated (IDE, 2009). This trend of groundwater irrigation is unplanned, and it is expected to cause a decline of the groundwater level in the region, as well as pumping of natural arsenic contamination, water being harder to access and more costly to lift and negative effects on suction pumps. Also, the other option, increased access to/ use of surface water in Cambodia, is not favourable, as it reduces the flow downstream and thus, lowers the water level

in Vietnam's irrigation channels. As both consequences need to be avoided, irrigation pattern and groundwater use must be carefully studied to understand the hydraulic consequences when fulfilling the irrigation demand during the dry season (Erban and Gorelick, 2016).

Groundwater is used in agriculture in southern and eastern Cambodia, but not in the northeast, even though groundwater at lower depth (50-70 meters) is available in both, southern and north-eastern parts of Cambodia. In the lowlands in the Mekong basin, farmers can install shallow tube and dug wells to water dry season crops, which would otherwise be prone to fail due to the lack of water in the dry season. These wells are known to be installed in 7 of the 14 provinces: Battambang, Kampong Cham, Kampong Chhnang, Kandal, Prey Veng, Siem Reap, and Takeo (Oeurng, 2020). The provinces Prey Veng and Svay Rieng (Figure 1) are part of the Mekong Delta in the southeast of the country, characterized by the alluvial aquifer covering both, parts of Vietnam and parts of Cambodia. In these two provinces groundwater is increasingly extracted during the dry season. In Prey Veng, a province in the South- East, the installations of tube wells increased drastically from 1600 in 1996 to 25000 in 2005 (Oeurng, 2020).

In the last two years the irrigation pattern is expected to have changed due to various consequences of the Covid19 pandemic affecting agricultural activity. On the one hand, the Covid-19 pandemic caused Cambodians working predominantly in neighbouring Thailand, to return to their home country due to governmental restrictions (Barua, 2020). Another possibility is that farmers are no longer able to work in the town and return to the countryside to secure work in agriculture (UNDP Cambodia, 2020). Furthermore, Cambodian farmers are facing economic challenges and are at risk of falling into depths (Keng and Rim, 2021). The price of paddy rice and other crops was dropping during the pandemic years, due to less demand and less rice customers (The Phnom Penh Post, 2021). It is unknown, how the economic challenges that farmers have been facing has changed agricultural land use, and groundwater usage for irrigation in agriculture.

Changes in irrigation pattern were examined in a remote sensing analysis on Normalized Difference Vegetation Index (NDVI) and evapotranspiration (ET) in the framework of a project course in the autumn semester 2022. Results from the NDVI remote sensing analysis showed that during the pandemic years,

extensive areas were switching from being irrigated to non-irrigated, but also switching back again eventually during these years. Results of this study are presented in the background, in section 2.7.

This study is following up the remote sensing study, determining the hydrologic impact of the water storage in the aquifer of changing groundwater use for irrigation in south-eastern Cambodia. The study area for the groundwater model is further reduced to Prey Veng and Svay Rieng, where groundwater observation wells, supported by the EU-funded PRASAC programme, exist. This region also covers 10 % of the rice cultivation of Cambodia (Erban and Gorelick, 2016). The study is going along with a bigger study by the International Water Management Institute (IWMI), the National University of Laos and the Institute of Technology Cambodia (Financial Support: SUMERNET / SEI), evaluating sustainable and inclusive groundwater use for agriculture in the lower Mekong region.

1.1 Aim and objective

The aim of this study is to receive a comprehensive overview of the groundwater resource in terms of quantitative change during the pandemic, with relation to the changes in irrigation, which were examined in the project course. Thereby, the objective is to create a groundwater model displaying the hydrogeological situation of the groundwater resource and relating the outcomes of the irrigation study to the groundwater model. Since groundwater data is on the one hand limited and on the other hand not easily accessible in Cambodia, a field visit to the study area with the duration of two months is planned to collect missing data from stakeholders and measure the most recent water level in Prey Veng and Svay Rieng.

The objectives are as follows:

- collect necessary data (recent and historical water levels, stratigraphy of the layers, validation data for the remote sensing study) on a field study in Cambodia
- build a steady state groundwater model that covers the observation wells in Prey Veng and Svay Rieng in GMS MODFLOW
- extent the steady state groundwater model to transient state using monthly input data (calibration period: April 1996 to December 2008; validation period: January 2015 to March 2022)
- relate changes in groundwater irrigation seen in the remote sensing analysis (see chapter 2.7) to consequences on the groundwater storage by applying the Evapotranspiration package in GMS MODFLOW together with an automated parameter estimation algorithm PEST

2. Background

2.1 Study area

The study area that is modelled for, includes the two provinces in the southeast of Cambodia, Prey Veng and Svay Rieng, seen in **Figure 1**, and it extents further towards the hydrological boundaries which are further described in Chapter 3.3.1. The area in south-eastern Cambodia is characterized of low-lying elevations, made of alluvial quaternary deposits, consisting of clay sand and gravel (see Chapter 3.3.2).

Cambodia has two seasons, a dry season in between November and April, and the wet season between May and November. The annual rainfall is ranging between 1400 and 1700 mm (Kogyo, 2002).

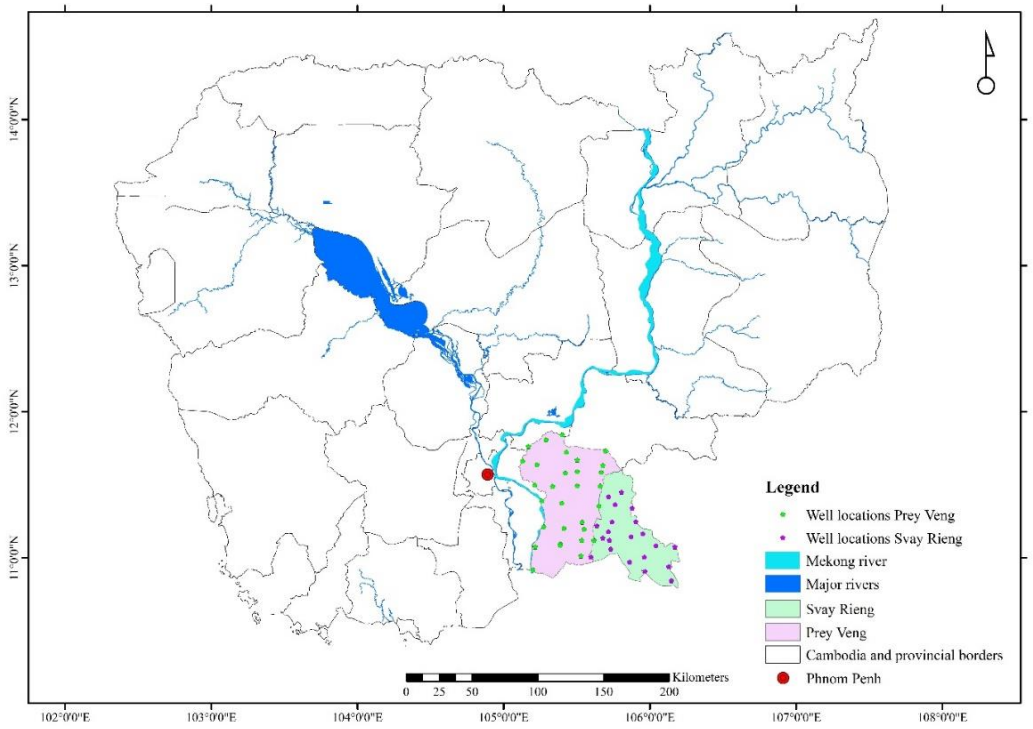

Figure 1: *Map of Cambodia with major rivers and provincial borders. Marked are the provinces Svay Rieng and Prey Veng, where the observation wells are situated. Source: Open Development Cambodia and IWMI (n.d.).*

2.2 Rice cultivation

In Cambodia, rice is the governing crop produced on agricultural land, occupying 75 % of the cultivated area, and it is exported to mainly neighbouring countries such as Thailand and Vietnam for milling, local distribution, and further export (IFC, 2015). Rice can be cultivated in both seasons, however, the limited rainfall in the dry season and low water levels in surface water bodies make it necessary to withdraw groundwater from aquifers in order to succeed with the rice crop. During the last decade rice production has been drastically increasing, as seen in **Figure 2**: While it was 4 million metric tons of paddy rice produced in 2000, in 2016 the production increased to an estimated 9.9 million metric tons (**Figure 2**) (FFTC-AP, 2018).

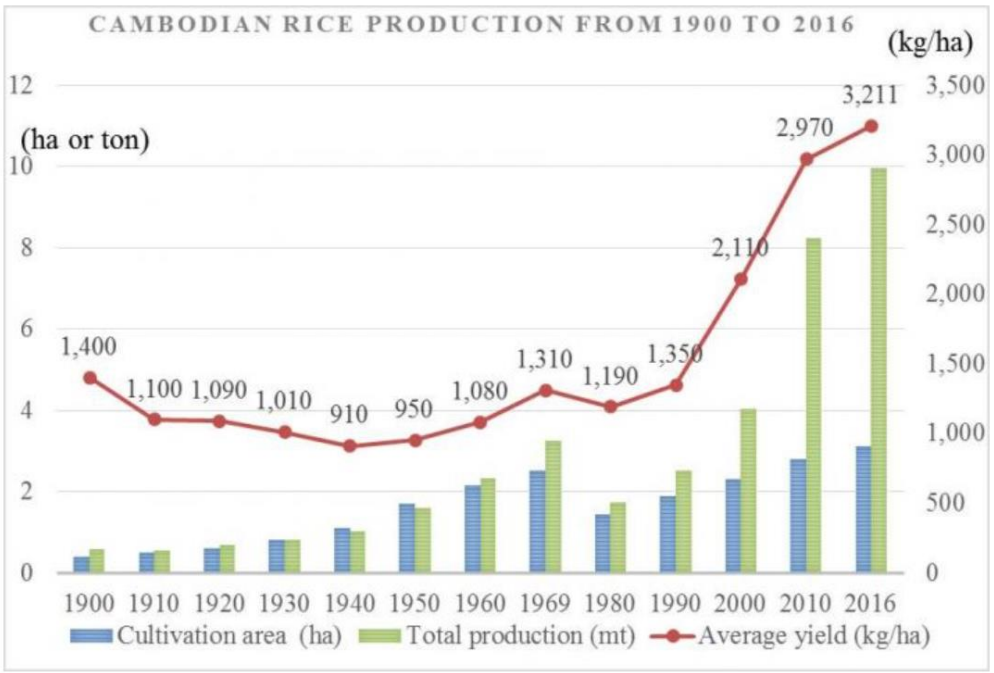

Figure 2: *Rice cultivation (ha), total production (mt) and average yield (kg/ha) between 1900 and 2016. Source: FFTC-AP.*

2.3 Groundwater usage

Groundwater is used for drinking water supply and irrigation purpose in Cambodia. During the dry season, half of the population is supplied with groundwater. Most households in Prey Veng and Svay Rieng use borehole wells with simple suction hand pumps, the wells can be easily and

inexpensively accessed. Those pumps can withdraw water until a depth of 6 m. This means if the groundwater table is lower than 6 m, then devices, such as positive displacement or mechanized pumps are needed to withdraw water from deeper parts. These devices are much more expensive and often not affordable by the farmers. During the dry season the groundwater provides partial irrigation. In agricultural areas that are distant from a surface water source or an irrigation system, groundwater usage is crucial for the success of the dry season crop. In the Mekong lowlands, where the provinces Prey Veng and Svay Rieng are situated, the aquifers are shallow and can be easily reached by installing dug and tube wells that to withdraw groundwater (Chantas report).

Wells have been used for domestic water supply in the past, without severe consequences on the water resource. However, the usage of groundwater for irrigation is growing rapidly and unregulated (IDE, 2009). Most of the land in Prey Veng and Svay Rieng is used for agriculture (**Figure 3**), mainly cultivating rice. Parts of Prey Veng and Svay Rieng have easily accessible groundwater which is withdrawn for irrigation from flush-bored wells and diesel pumps. Through unpredictable rainfall during the rainy season, the crop is at a risk to fail. Groundwater irrigation instead, results in higher rice yield, desertification into other crops and income and is easily controlled with adjustment of the pumping rates and time of application. Reports show that the domestic water supply wells nearby the pumping for irrigation are becoming dry, while the long-term consequences on the resource remain unclear (IDE, 2009).

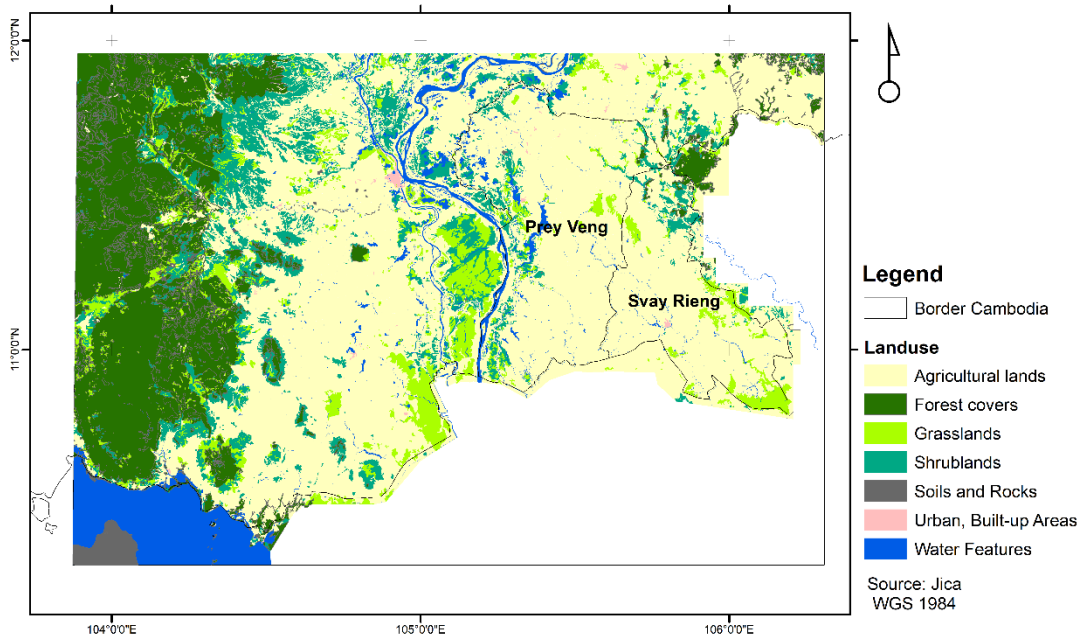

Figure 3: *Landuse in southeast Cambodia, mainly being characterized by agricultural lands. Source: Kogyo, 2002.*

2.4 Declining groundwater levels

IDE (2009) found that there is a declining trend of groundwater levels, seen at the observation wells in Prey Veng and Svay Rieng, between 1996 and 2008. The steepest decline is between Prey Veng and Svay Rieng, and the lowest decline is found close to the Mekong River. This change in water level over short term can either be naturally and climatically caused or be manmade. The risk of water levels falling below 6 m is high and it is already seen in data from 2008. With a drawdown of more than 6 m, the surface mounted suction pumps will not be able to pump anymore and threaten the rural drinking water supply. It would be necessary to replace the more than 13.000 suction pumps with positive displacement pumps that can reach greater depths, however, as stated earlier this would be too pricey for the rural communities (>100 $) (IDE, 2009). Erban and Gorelick (2016) found that groundwater use is rising with 10 % per year. This would also mean that the groundwater levels would fall below the limit of pumping in less than 15 years (Erban and Gorelick, 2016).

2.5 Existing Models and earlier studies

IDE established a groundwater model covering Prey Veng and Svay Rieng and extending further to towards the Mekong River in the west and south, and water divides in the east and north, thereby stretching into large parts of Vietnam (IDE, 2009). The study presents a long-term sustainable withdrawal rate for a drawdown limit of 6 m, however, the utilized withdrawal rates on site were unclear, so it was difficult to put the numbers into context. The model gives an understanding of groundwater flow in southern Cambodia, but usage for future predictive scenarios caution needs to be practised (IDE, 2009). This is because of uncertainties in properties such as the hydraulic conductivity of the Old Alluvium. The values of hydraulic conductivity were determined by calibration and may not refer to reality.

Another groundwater model in southeast Cambodia was established by Erban and Gorelick (2016) in combination with a remote sensing study on irrigation, giving major key guidelines for this study. It was found that groundwater-irrigated land increased at a rate of above 10 % per year in the Cambodian Delta region and points out the vulnerability of the water resource when irrigation activity further expands. Analysis of the groundwater model showed that even with a best-case scenario meaning the scenario with the least possible pumping, certain areas would result in wells being dry around the year, within five years, as visualized in **Figure 4** (Erban and Gorelick, 2016). Five years have passed now, thus, it will be interesting to see the results of this study.

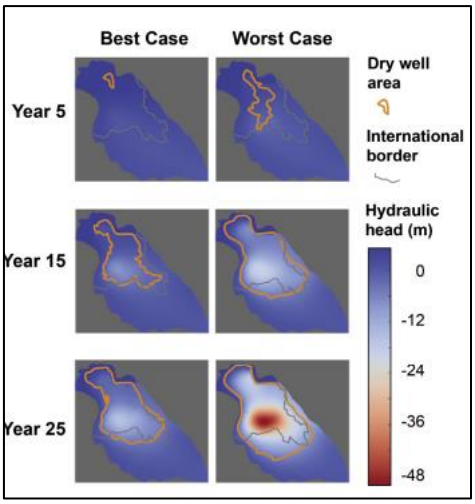

Figure 4: *Simulated scenarios from the study from Erban and Gorelick (2016). Best (left) and worst (right) case scenarios for aquifer hydraulic heads (elevation of the water table), during a 25- year long simulation period.*

A third model in development is the NexView model, by the United States Geological Survey (USGS). This numerical Modflow model focusses on a study area further to the west compared to our model and covers only few parts of Prey Veng (Davis, 2020).

2.6 Groundwater flow

Information on groundwater flow is very limited and highly uncertain in the study area. Studies suggest that recharge from rainfall is possible in the northern part of the modelled area (IDE, 2009; Erban and Gorelick, 2016), and affects the dominant flow direction going from the recharge areas in the North towards the south of the study area. Furthermore, a hydraulic connection between the Mekong River in the North of Prey Veng and the aquifer is possible, affecting the southward flow. This dominant flow condition was concluded from Roberts (1998) study analysing groundwater elevations. Roberts further concluded that the water levels in the area close to the Mekong River are affected by the river levels which are varying seasonally. Several studies assumed a seasonal variation in the groundwater flow direction: During the dry season the water level of the Mekong River is low, thus, groundwater from the aquifer flows westwards and discharges into the river. During the wet season when the head stages in the Mekong River are high, the Mekong

recharges the aquifer and groundwater flow is eastwards into the aquifer instead (Roberts, 1998; IDE, 2009).

2.7 Irrigation changes during the pandemic

Irrigation changes during the dry season (beginning of December to the end of March, for the seasons in between December 2016 and March 2021) were examined by a remote sensing analysis of NDVI and ET during the autumn semester. NDVI was chosen to be looked at as it is a general indicator of vegetation growth, and the study area mainly covered agricultural land with rice cultivation (**Figure 3**). Water sources of ET can either be rain, surface water or groundwater used in irrigation practices. It was looked at the dry season, where surface water bodies are not abundant and do not have a significant effect on evapotranspiration. Rainfall is rare during the dry season and analyses of correlations between rainfall and ET, did not show an obvious and significant correlation, thus, it was concluded that there are other driving factors, such as groundwater irrigation determining ET amount in the dry season. This is why ET was chosen to be analysed as an indicator for groundwater irrigation. This further supports the idea of ET being an indication of irrigation amount in the dry season.

Looking at the NDVI analysis, **Table 1** shows the irrigation changes comparing the dry season of one specified year to the dry season in the following year, depicted in percentage of area. These changes are visualized in **Figure 5**, **Figure 6**, **Figure 7** and **Figure 8**. Looking at the change 2018/19, representing the pre pandemic situation, to one year later in 2019/20. **Figure 7** shows that there is a big extent of area changing from irrigation to non-irrigation. This can be a result of the low rainfall; however, it is likely that the pandemic has shown consequences on the farmer's life. The drop in rice price can be related to the change from irrigation to non- irrigation, when farmers did not earn enough from rice production (Camboja News, 2021). Comparing with ET, it showed moderate and not much changing values in 2018/2019 and an increase in December and January, followed by a steep decrease, which may be related to the switch to non-irrigation. The more equal distribution in NDVI analysis between areas that changed from non- irrigated to irrigated and from irrigated to non- irrigated looking at the change between 2019/20 and 2020/21 (**Figure 8**), suggests that people who lost their jobs in town, due to local and travel restrictions, come back to the countryside to receive some income with farming. Comparing pre- pandemic and post-pandemic conditions, however,

in **Figure 9:** Results from the remote sensing analysis showing the change between 2018/19, depicting the pre-pandemic situation, and 2020/21 during the pandemic: Non- irrigated in 2018/19 to irrigated in 2020/21, irrigated in 2018/19 to non- irrigated in 2020/21 and no change between those two dry seasons. The pie chart shows the categories as percentage of area (see also Table 1)., it is visible that the switch to non- irrigation prevails extensively.

It was rather difficult to relate ET and NDVI, as the NDVI analysis was made for the complete dry season, and it cannot be specified at which month the limit to category 'irrigated' or 'non-irrigated' was crossed. The ET mosaics were created for one day every month, where some of the scenes could have one day difference in capturing date.

It was originally planned to use the ET images that were produced from Landsat Data using the GEE Sebal algorithm, as an input to the groundwater model. However, the produced mosaics from the different Landsat scenes were often mismatching and also had a high cloud coverage. This is shown in **Figure 10**. Instead, the evapotranspiration was calibrated for when running the transient state model and then compared to the images produced by the remote sensing analysis of ET and NDVI.

Table 1: *Irrigation change depicted as percentage of total land area.*

	No change (%)	Non-irrigated to irrigated (%)	Irrigated to non-irrigated (%)
Change 19/20 to 20/21	88,42	5,55	6,04
Change 18/19 to 19/20	84,60	2,22	13,19
Change 17/18 to 18/19	90,22	4,12	5,66
Change 16/17 to 17/18	94,07	3,30	2,64
Change 18/19 to 20/21	84,62	1,96	13,42

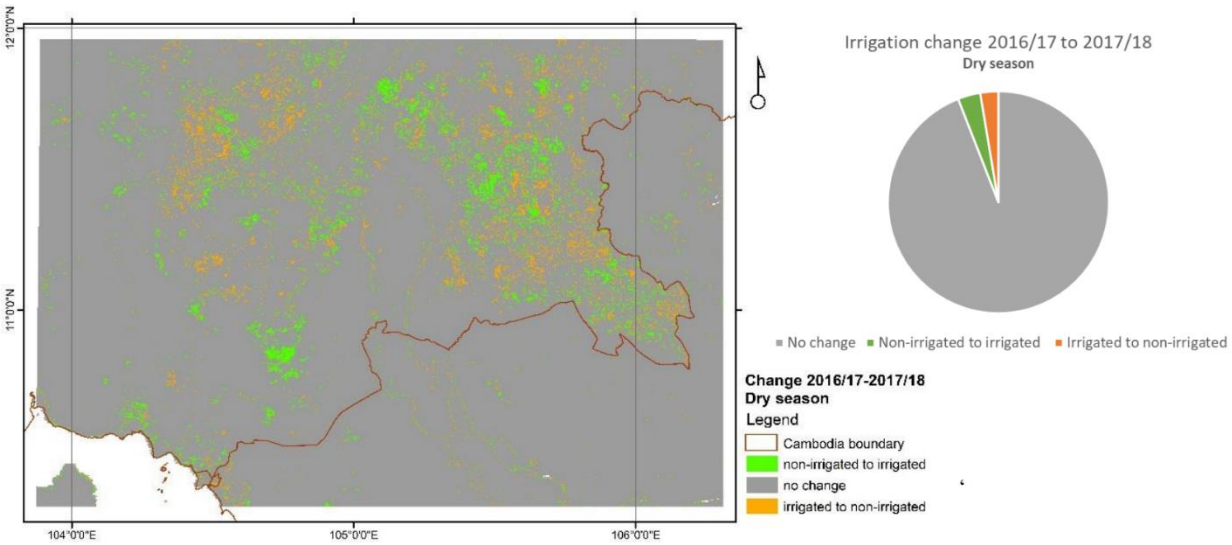

Figure 5: *Results from the NDVI remote sensing analysis showing the change between 2016/2017 and 2017/2018: Non-irrigated in 2016/17 to irrigated in 2017/18, irrigated in 2016/17 to non- irrigated in 2017/18 and no change between those two dry seasons. The pie chart shows the categories as percentage of area (see also Table 1).*

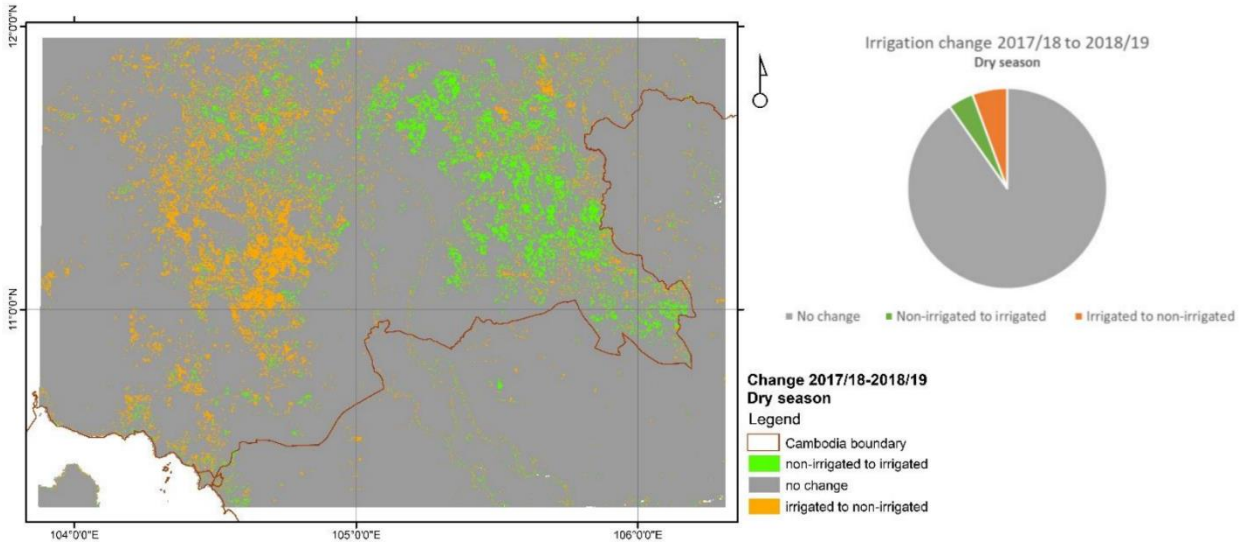

Figure 6: *Results of the NDVI remote sensing analysis showing the change between 2017/18 and 2018/19: Non- irrigated in 2017/18 to irrigated in 2018/19, irrigated in 2017/18 to non- irrigated in 2018/19 and no change between those two dry seasons. The pie chart shows the categories as percentage of area (see also Table 2).*

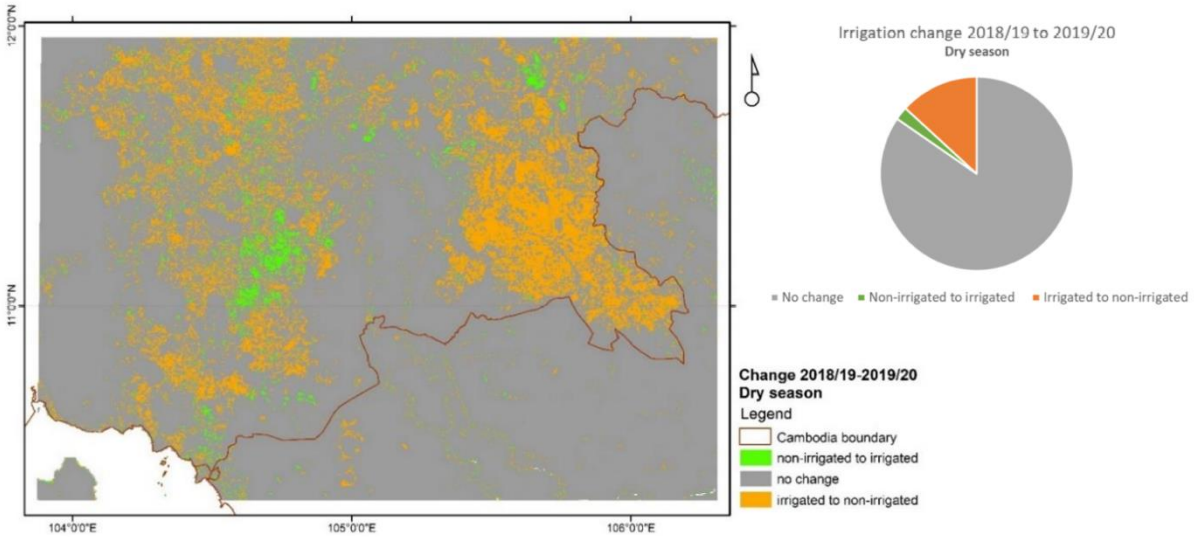

Figure 7: *Results of the NDVI remote sensing analysis showing the change between 2018/19 and 2019/20: Non- irrigated in 2018/19 to irrigated in 2019/20, irrigated in 2018/19 to non- irrigated in 2019/20 and no change between those two dry seasons. The pie chart shows the categories as percentage of area (see also Table 1).*

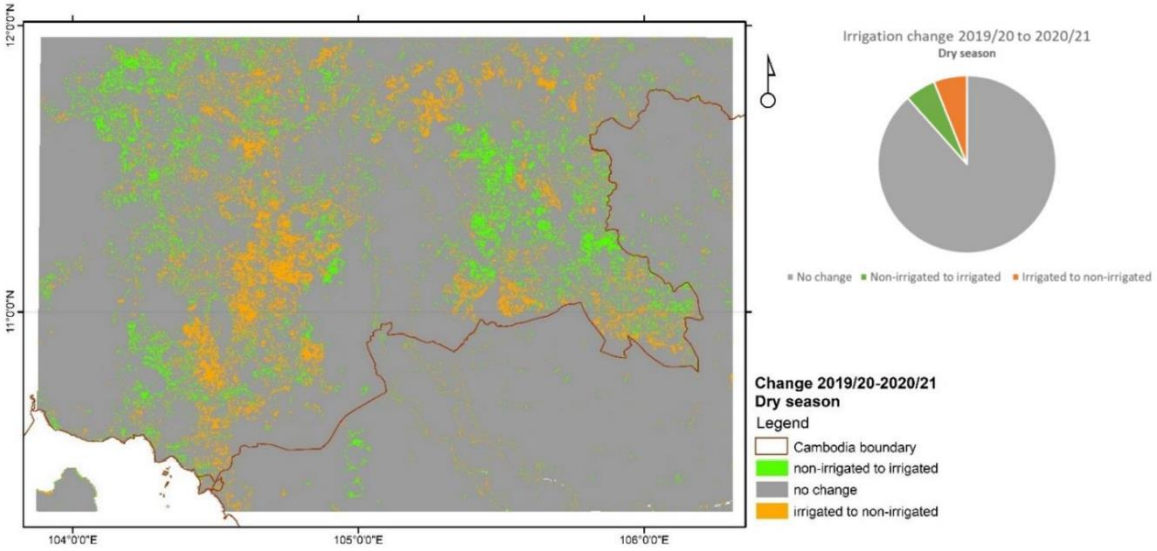

Figure 8: *Results from the NDVI remote sensing analysis showing the change between 2019/20 and 2020/21: Non- irrigated in 2019/20 to irrigated in 2020/21, irrigated in 2019/20 to non- irrigated in 2020/21 and no change between those two dry seasons. The pie chart shows the categories as percentage of area (see also Table 1).*

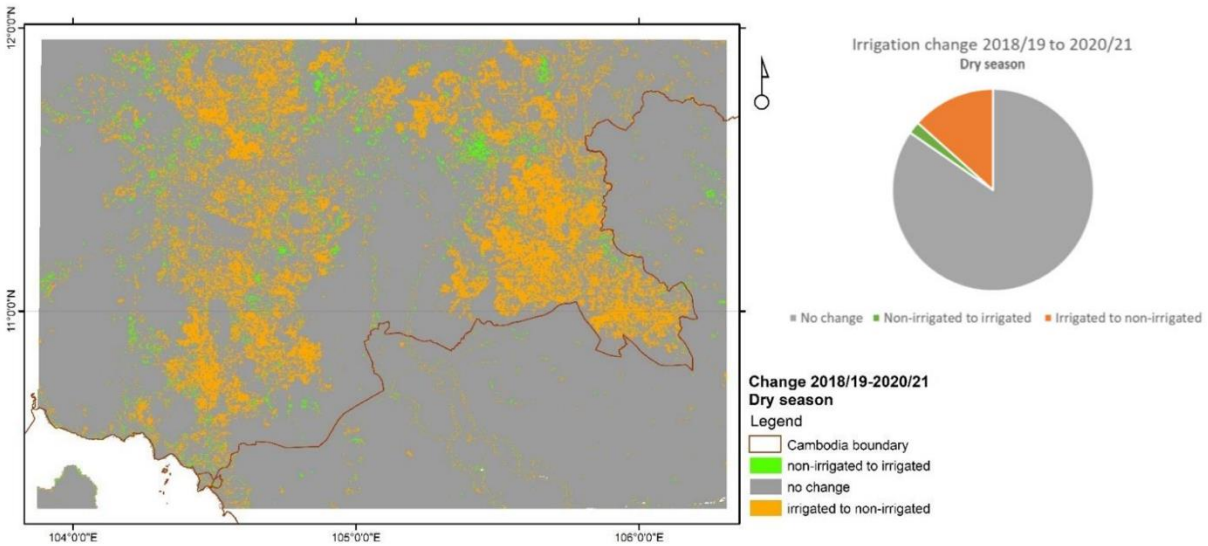

Figure 9: *Results from the remote sensing analysis showing the change between 2018/19, depicting the pre-pandemic situation, and 2020/21 during the pandemic: Non- irrigated in 2018/19 to irrigated in 2020/21, irrigated in 2018/19 to non- irrigated in 2020/21 and no change between those two dry seasons. The pie chart shows the categories as percentage of area (see also Table 1).*

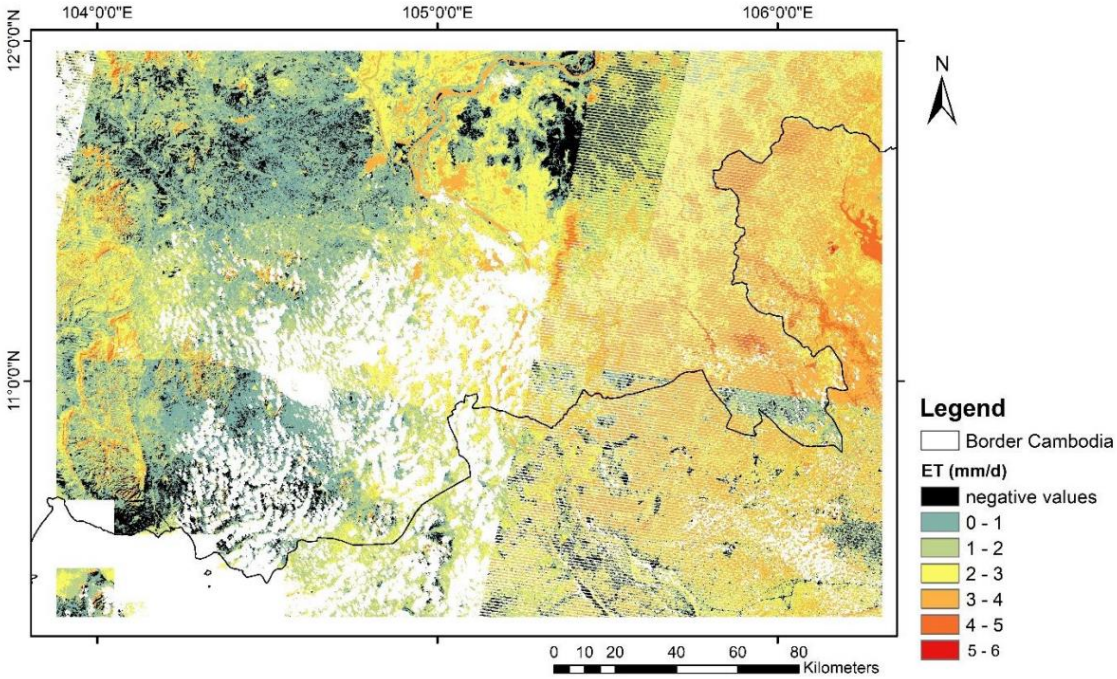

Figure 10: *Image mosaic, with mismatching scenes, using default percentiles, containing images from 1st and 2nd of December 2018. Negative values are seen in black; they were eliminated for the further study. White colours represent presence of clouds that were masked out.*

3. Methodology

There are five steps to be taken in order to create a groundwater model: data collection, conceptualization, simulation, calibration and verification (Hashemi et al., 2012). The geological and hydrogeological data of the study area was collected by talking to stakeholders on a field visit and measuring the water level, and it was also obtained by related literature. ArcGIS Desktop 10.5.1. is a desktop application for mapping and analysis of spatial data produced by ESRI (Esri, 2020). In this study it was used for creating maps and interpolating data spatially. The second software that was most relevant for this study was GMS MODFLOW 9.0.5 produced by the engineering company Aquaveo and the most intuitive and quick groundwater modelling software available. With GMS MODFLOW three- dimensional models can be established, using GIS objects and other various source data types.

3.1 Description of Models

3.1.1 Conceptual Model

A conceptual model was established for better understanding of the hydrogeologic situation. With that understanding it is possible to determine boundary conditions to define the area that is hydrologically influenced by the well extraction. The conceptual model was created using AdobeFresco (2018) and ArcGIS Desktop 10.5.1.

The aquifer characterizing Prey Veng and Svay Rieng is the most productive one in Cambodia and stretches into the Mekong delta region of Vietnam (Erban and Gorelick, 2016). It is characterized by low elevations (**Figure 14**) where parts of it can be flooded from the Mekong River during the rainy season. Two broad sedimentary layers can be defined regarding aquifer material: The upper layer, consisting of fine-grained silts and clays, has a depth of 10 to 40 meter and is referred to as young alluvium. Seen in **Figure 11** is that the surface geologic layer in the southeast is characterized by this young alluvium, compared to other parts of Cambodia which have various other types of rock origins. This young alluvium does not allow much water to infiltrate and recharge the aquifer, but instead, annual flooding is likely to happen. The lower layer, consisting of coarse-grained sand and gravel, is called old alluvium and characterizes a good aquifer, being 200 m thick and even more. The information on the deep aquifer is very unknown and not available. Though JICA (Kogyo, 2002) has published a map with estimated bedrock depths,

which has been further used to define the depth of the lower layer (see 3.3.3 Geologic layer elevations). The cross sections in **Figure 12** and **Figure 13** represent the section A-A' and B-B' respectively, as indicated in zoom of the geology map (**Figure 11**).

Figure 12 of cross section A-A' shows that the aquifer (old alluvium) is situated in between bedrock reaching higher levels in the East, or even outcropping in the West. The eastern boundary can thus be defined by the bedrock approaching the surface as the flow will be limited there. The cross section also depicts the Mekong River, being a water divide that can define the western boundary. The boundary conditions are further described in Chapter 3.3.1 Boundary **Figure 13** shows the cross-section B-B' showing the bedrock ranging between -200 and -50 m. This map was based on **Appendix 2** and **Appendix 4** from IDE, where **Appendix 4** has also been used to define the bedrock further (Chapter 3.3.3 Geologic layer elevations). It is visible from both cross sections that the western and southern part is characterized by a confining layer, while the aquifer (old alluvium) reaches the surface in the north- eastern part.

The south-eastern tip of Svay Rieng has elevations of 1 to 3 m and has underlaying young alluvium which is further extending into Vietnam. Most province has elevations of 3 to 15 m and has silt and clay soils, with low infiltration, which are underlain by old alluvium (Rasmussen, 1977). Prey Veng is characterized by a low laying plain with elevations around 2 m in the south and around 13 m in the northern parts. It is assumed that the Mekong River is deep enough to be able to recharge (rainy season) and also discharge (dry season) the lower layer of old alluvium. The upper young alluvium layer acts as a confining layer, thus no recharge to the lower is happening through the layer as indicated in **Figure 12** and **Figure 13**.

According to Erban and Gorelick's findings, the hydraulic response by irrigation pumping is insignificant at regional scale through the year 2008 where their available observations end. Instead, the hydraulic response was determined by natural forcings such as the transient stage of the Mekong. It did not show seasonal oscillations in hydraulic heads in wells in further distance. Erban and Gorelick accounted for those refinements by adding recharge, despite recharge by rainfall is negligible in the largest part of the modelled area, as most of it is lost by evapotranspiration or further kept by the aquitard,

not reaching the aquifer but leading to flooding instead (Erban and Gorelick, 2016).

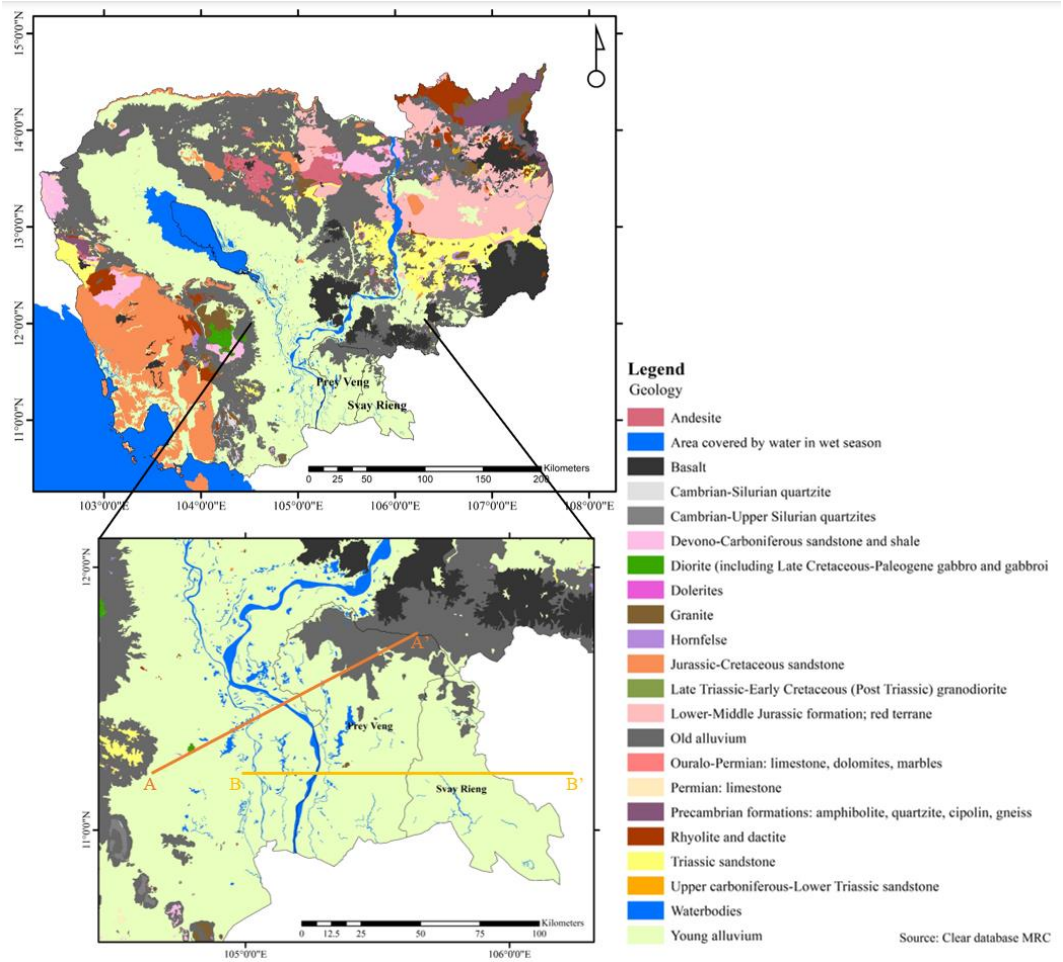

Figure 11: *Surface geology of Cambodia and zoom in to study area which is characterized by surficial Young Alluvium.*

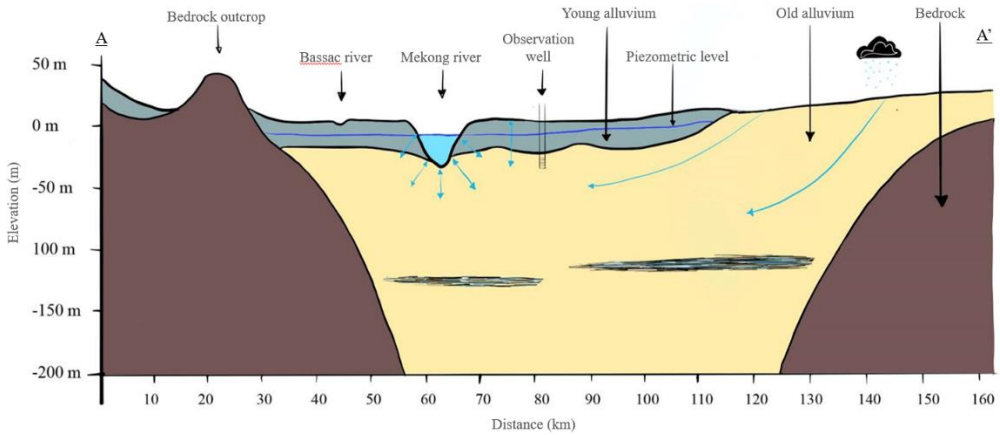

Figure 12: *Cross section A-A`.*

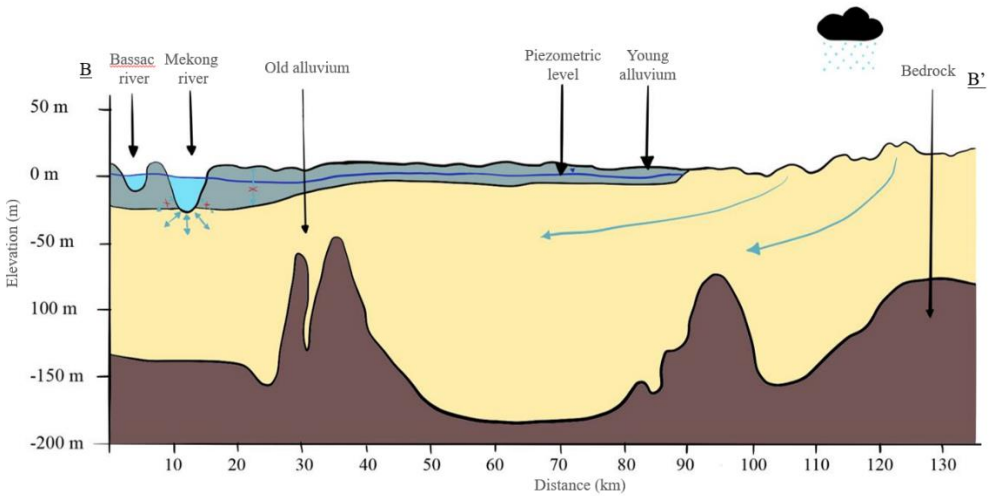

Figure 13: *Cross section B-B`.*

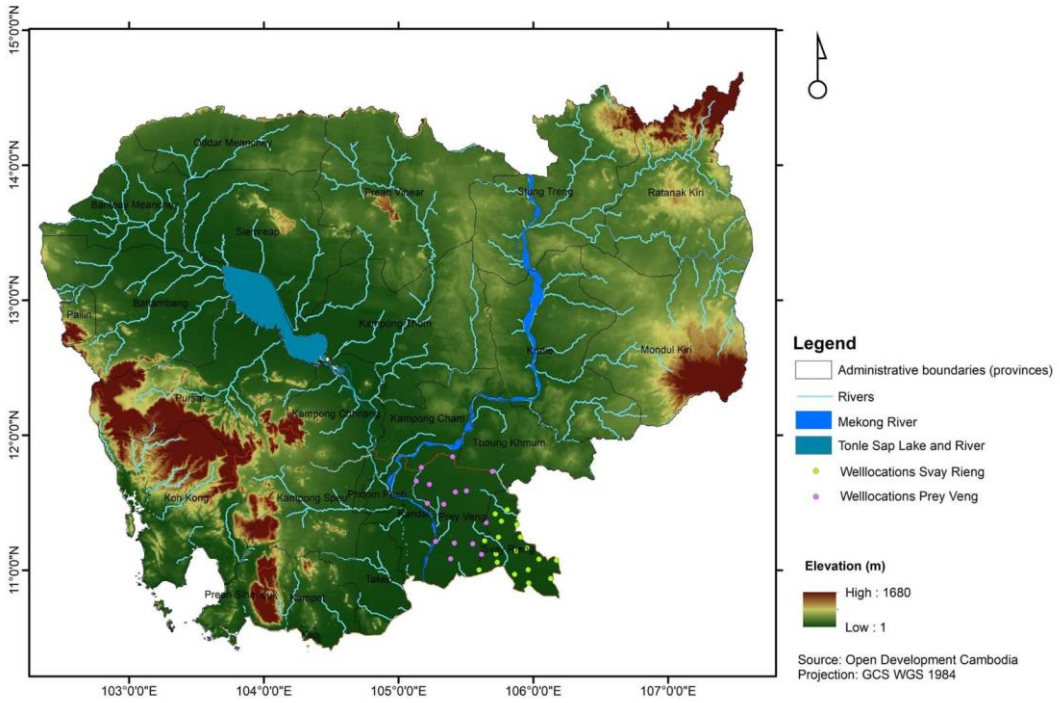

Figure 14: *DEM of Cambodia and observation wells, with low elevations in the southeast of Cambodia.*

To simplify hydrogeology for the modelling process, several assumptions have been made and were followed when creating the steady state and transient state model with information based on the conceptual model:

- Isotropic hydrogeologic conditions were assumed within one geologic layer (aquifer or aquitard)
- Specific storage is a characteristic for confined conditions and greater for clays due to their compressibility, and it was assumed to be homogeneous within each layer
- The specific yield, a characteristic for unconfined conditions and with greater values for sands as the texture is more drainable, was also assumed homogeneous for each layer
- Time units were set to monthly, in accordance with the monthly format of observation well data
- Elevation data for the different layers was only available for certain points, thus, layer elevations were spatially interpolated

3.1.2 Steady state model

In order to have fewer unknown parameters to calibrate for, a steady state model was developed and run in GMS MODFLOW 9.0.5. In a steady state model, the vertical water movement is not relevant, it only considers the horizontal change. Thus, the specific yield and specific storage parameters are not included in the model, giving the possibility to have only the one unknown parameter of hydraulic conductivity to calibrate for. As water was lacking in the steady state model, recharge was added to the zone where the permeable old alluvium reaches the surface. This was done according to IDE (2009)'s study, who also included recharge in their steady state model.

From the available groundwater level data, the steady state condition was determined by firstly averaging the measurement of one-time step (month) for all stations, then taking the actual difference between the means for each time step, i.e. the actual difference between the mean at time 1 and at time 2, the actual difference between the mean at time 2 and time 3, and so on. Then the mean between two consecutive actual differences was taken. If this mean was below 0.25 it was considered as a steady state condition. Chosen to represent the steady state condition was the March 2006, laying within a period of steady state condition. The groundwater level observations for March 2006 were inserted into the model, together with river heads for the same month, and other model parameters as described in chapter 3.3 Data inputs.

3.1.3 Transient state model

The transient model was also established in and run in GMS MODFLOW 9.0.5, where stress periods were defined according to the available data. Due to the groundwater level data, which was given on a monthly basis, the time discretization in the model was monthly. The additional factors of storativity, specific storage, pumping and evapotranspiration were added into this model, as they determine the vertical transport of water through the soil layers. The model was set up for calibration purpose using automated parameter estimation with PEST, from April 1996 to December 2005 and for validation purpose from January 2006 to December 2008. Then it was run for pre- pandemic (January 2015 to December 2019) and pandemic time (January 2020 to March 2022), also using PEST.

3.2 Data collection in Cambodia

The data collection was carried out during 2 months in Cambodia. I closely collaborated with the Institute of Technology in Cambodia (ITC) in Phnom Penh, they offered me a place to work in their office and a few students supported my work in the provinces. The data collection in Cambodia consisted of three parts/activities: One field visit in Prey Veng, one field visit in Svay Rieng and several talks with NGOs and ministries/ provincial departments. Also, the direct contact to the ITC was very helpful, due to language barriers and for orientation in the country. After arriving in Phnom Penh, several days were needed for organisation of the first field trip, but also for orientation in the capital, getting to know the students who offered me help and the staff at ITC.

To establish a groundwater model, data on ground water levels were collected in Prey Veng and Svay Rieng, where 49 wells were installed by the EU funded PRASAC programme to monitor water levels.

Objectives of the data collection were to visit all wells in Prey Veng and Svay Rieng to check availability/maintenance and measure water levels, and request water level data from the Provincial Departments of Water Resources and Meteorology in Prey Veng and Svay Rieng. Furthermore, it was aimed to receive first hand data on for example stratigraphy and river head data.

3.2.1 Activity 1- Data collection in Prey Veng

Participants were Svea Bertolatus from Lund University/IWMI, Chanseyma Khoeun and Penglong Koun from the Institute of Technology Cambodia, and a driver. The field visit to Prey Veng was scheduled for three days, 15th to 17th of February 2022. Our team started very early at ITC Phnom Penh, with a reliable driver and car, to visit as many wells as possible during the day. For the first day the wells in the north of Prey Veng were planned to be visited. A device was brought from Lund University, but it failed to take measurements. After several tries to repair and discussions on how to continue, it was chosen to continue with an alternative method, using measurement tape and a fish lamp. The method worked well, and it was possible to visit a few wells and take measurements with this alternative method. Seen along the paths were many rice fields using groundwater irrigation. The team stayed for the night in Prey Veng.

The next morning started relatively early, to visit one well at the Provincial Department of Water Resources and Meteorology, and also use this opportunity to talk to the responsible officer in the department, Heng

Bunthoeun, who was very welcoming and could provide data and information on the wells. A few outcomes of the talk were:

- Water level data from 2015 to 2021 can be provided
- The water level is seen to be declining year by year, when plotting the data in excel
- The water supply is reliant on the groundwater right now, however, there is a contract established with World Bank to stop using groundwater for supply by 2025
- Stratigraphic logs of certain wells may be available

The officer also provided another water level meter for our team to borrow during this field visit. After the visit in the department, the team continued the measurements at the observation wells, and thereby visited the wells located in the centre parts of Prey Veng province, before reaching Neak Loeung to stay for the night.
Also, the third day started early to reach as many wells as possible, this time in the south of Prey Veng province. The roads were difficult to drive, it took time to reach the wells. In the later afternoon, the team met the officer in Prey Veng once again, to receive ground water level data and return the device. Then it was time to return to Phnom Penh. In total 24 well locations were visited, where 17 were available to take measurements from.

3.2.2 Activity 2- Data collection in Svay Rieng

Participants were Svea Bertolatus from Lund University/IWMI, Attitya Mom and Penglong Koun from the Institute of Technology Cambodia, and a driver. The second visit was scheduled for two days, 25th and 26th of February 2022. Again, the team started early in Phnom Penh for the 3-hour journey to Svay Rieng. On the way, Prey Veng was passed, to borrow the water level device another time to do the measurements in a quick and efficient way. A few measurements were taken before reaching the Provincial Department of Water Resources and Meteorology in Svay Rieng. The official person was not available on this Friday afternoon, however, the officer talking to our team provided the contact and it was possible to get in touch with him via Telegram. He promised to send the water level data from 2015 to 2021 as soon as possible. After the visit the team continued to measure water levels at the wells in the southern parts of Svay Rieng. There were only few wells where it was possible to measure, because most wells were closed for pumping and not accessible. The night was spent at Krong Bavet, right at the border to Vietnam.

At the second day the wells towards the north of Svay Rieng were visited, and this time much more wells were available to take measurements from. Around 16.00 all wells were visited, and it was time to go back to Phnom Penh, and returning the device on the way in Prey Veng. In total 18 wells were visited, of which only 8 were available for measurements.
The two trips to the provinces were very successful. We all were hardworking and managed to visit almost all wells.

3.2.3 Activity 3
After the two field trips, data was organised and more data on borehole logs was requested from the officer at the provincial department. He sent the data per post to the ITC, but it turned out to be consisting mainly of data on water quality which was not relevant for this study. I also visited several NGOs to get in contact with people who worked in the same field. The most successful was my visit to the iDE Cambodia in Phnom Penh, and the following meeting with Michael Roberts, who has been conducting several groundwater studies in south-eastern Cambodia and shared his data on stratigraphy (borehole logs), literature and more with me.

3.2.4 Conclusions of the data collection
The two field visits were only possible with our good work as a team, and the motivated and eager students and driver. The team turned the visits into very successful ones, visiting most of the wells that were accessible for measuring the water level, and receiving valuable data from the officers of the provincial departments. Visited NGOs were very open to support my work and provide the necessary data, share their deeper insights on the study topic.

3.3 Data inputs
The required data input for a groundwater model were (1) boundary conditions; (2) geology and soil properties of the aquifer layers (hydraulic conductivity, storativity); (3) geologic layer elevations; (4) river head data (5) observation wells (records of groundwater levels); (6) vertical recharge (rain) (7) vertical discharge (pumping) and (8) evapotranspiration. The starting head can be simulated with the calibrated model head of the steady state model based on groundwater level at the observation points in steady state, where results are shown in Chapter 4.1.2 Calibration results .

There are five main papers that have established groundwater models and hydrogeological investigations in the study area, and they are the main

reference for data taken from literature, for instance on specific storage, specific yield, recharge and hydraulic conductivity:

- Rasmusssen (1977)
- Roberts (1998)
- Kogyo (2002) (JICA)
- IDE (2005) and IDE (2009)
- Erban and Gorelick (2016).

3.3.1 Boundary

The easiest approach to set boundary conditions for the groundwater model was to choose specified head boundaries (zone in which the water levels are known through time) and no-flow boundaries (a zone with no groundwater flow, such as a groundwater divide).

Figure 15 shows a bedrock map of the study area with the major river and shows how the boundary proceeds. The Mekong River could be chosen as specified head boundary marking the boundary in the north, south and west from which water can recharge and discharge the aquifer but no flow underneath (IDE, 2009; Erban and Gorelick, 2016). The eastern boundary was set as no- flow- boundary at an abrupt elevation change from the lowlands with <10 m elevation to highlands with >20 m elevation, where the bedrock is coming close to the ground surface, as seen in **Figure 15** (Erban and Gorelick, 2016). Values for the head boundary were determined on a monthly basis. IDE (2009) assumed a groundwater divide with no flow conditions at the eastern boundary, though revised this assumption later and found that it is likely that discharge can happen along the eastern boundary into a trough diverting water into streams and rivers that flow towards the South China Sea and Vietnam (IDE, 2009). This study firstly ran the model with no flow conditions at the eastern boundary, but calibration was not satisfactory. Thus, the theory from IDE was adopted, modelling the middle part of the eastern boundary as a trough to which water discharges, while the northern and southern part of the eastern boundary kept the no- flow conditions. It was assumed that the part of the eastern boundary that allows discharge, is not significantly affected by seasonal variations.

The boundary part in the south is interfered from Anderson (1978) who mapped a saltwater- fresh water- interface in between Svay Rieng and the cost, which is used as specified head boundary with a head of 0.0 m representing

surface water bodies with water levels close to sea level where water from the aquifer can discharge to.
The extent of the boundary condition was the same for the steady state and the transient state model. However, there were differences when choosing head conditions for the Mekong River determining the boundary conditions in the West. The steady state model used the constant head stage from the time chosen as steady state, March 2006. These stages were slightly adjusted during steady state calibration as described in Chapter 3.5. For the transient model historical monthly data on head stages were used.

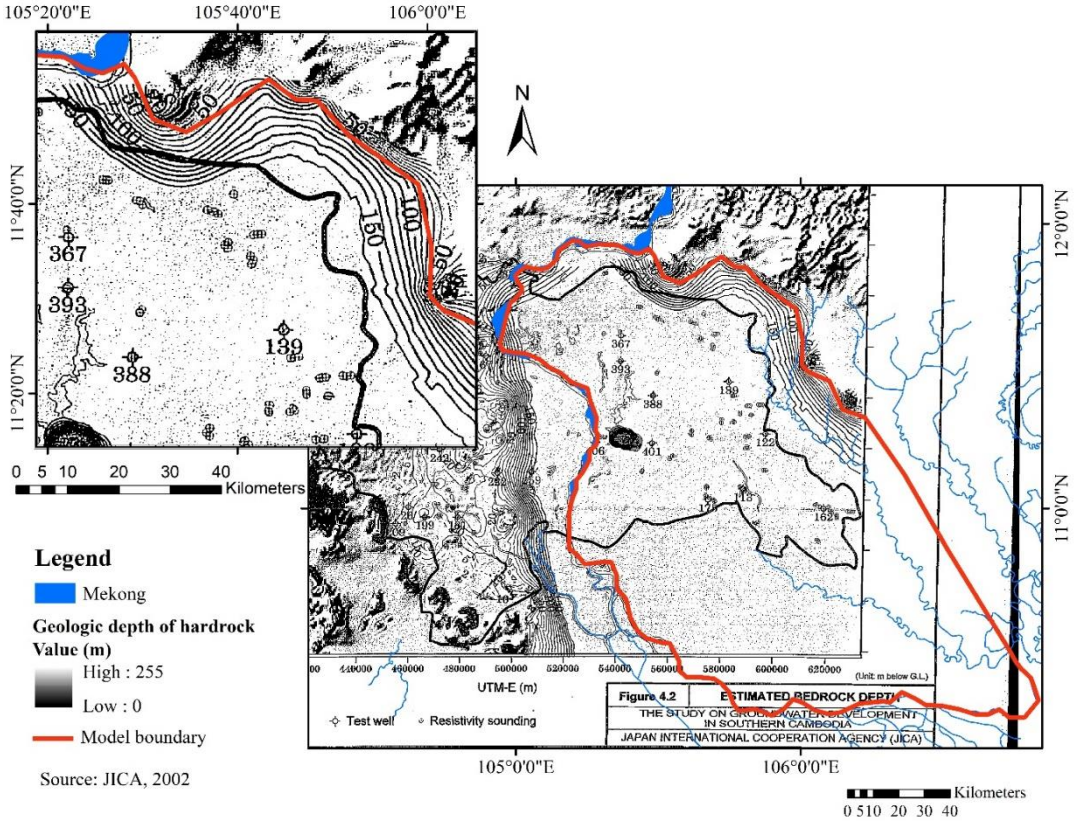

Figure 15: *Boundary conditions along the major river (Mekong River) and the bedrock approaching the surface.*

3.3.2 Geology and soil properties of the aquifer layers

- *Hydraulic conductivity*

Hydraulic conductivity K (unit: L/T), also called coefficient of permeability, describes the rate of water moving through a unit area of isotropic, permeable medium. Density and kinematic viscosity of the medium are important factors affecting K (Fetter, 2001; Rasmussen 1977). K is an important layer parameter to be specified in the MODFLOW simulation. A layer can be separated in several zones if the parameter varies spatially. K was assigned to the two geologic layers, whereas both layer were further divided into the zone that has a confining layer, and the zone that does not have a confining layer, resulting in four different K zones, seen in the schematic drawing in **Figure 16**. K1 is representing the confining upper young alluvium layer, K3 is the old alluvium

aquifer underneath, K4 is the lower old alluvium layer, without having the confining layer above, and K2 is describing the zone where the old alluvium reaches the surface.
Literature was used to know the range of reasonable K values for the different layers in the study area. There were several approaches done in order to determine reasonable and reliable K values. Roberts (1998) presented values of specific capacity from pumping tests in Svay Rieng and Prey Veng, meaning the ration of pumping rate and observed drawdown, which is an implication on potential short-term yield (IDE, 2009). From the correlation with specific capacity, transmissivity (T) values were approximated for 46 PRASAC wells (Roberts, 1998), however, the numbers are only a vague estimate, because it was not accounted for skin effects which are suggested to have some effect on the total drawdown. Yet, it is important to have a rough insight on the characteristics of the Old Alluvium and hence, the estimates of transmissivity are of importance. T average was estimated to be 3500 m2/d and assuming a aquifer depth of 200 m, this value would represent silty to clean sands (IDE, 2005). IDE (2009) used these T values from Roberts (1998) dividing T with the depth of the Old Alluvium layer in the respective location, to estimate K at 46 locations in the study area (Figure 13 in IDE report). After calibrating the IDE model, the aquifer values ranged from 0.13 m/d to 280 m/d. The most common value was 50 m/d describing the aquifer zones with different recharge input and confined but also unconfined layers (IDE, 2009). The K value of the confining layer was 8.6 $*10^{-3}$ m/d. Erban and Gorelick (2016) presented a K value of 8.64 * 10^{-4} for the aquitard. The aquifer had a value of 70 m/d, except a small zone in the North having middle and low K values, 7 and 0.7 m/d respectively.

K values within the ranges presented by literature were found during steady state calibration and presented in **Table 2**.

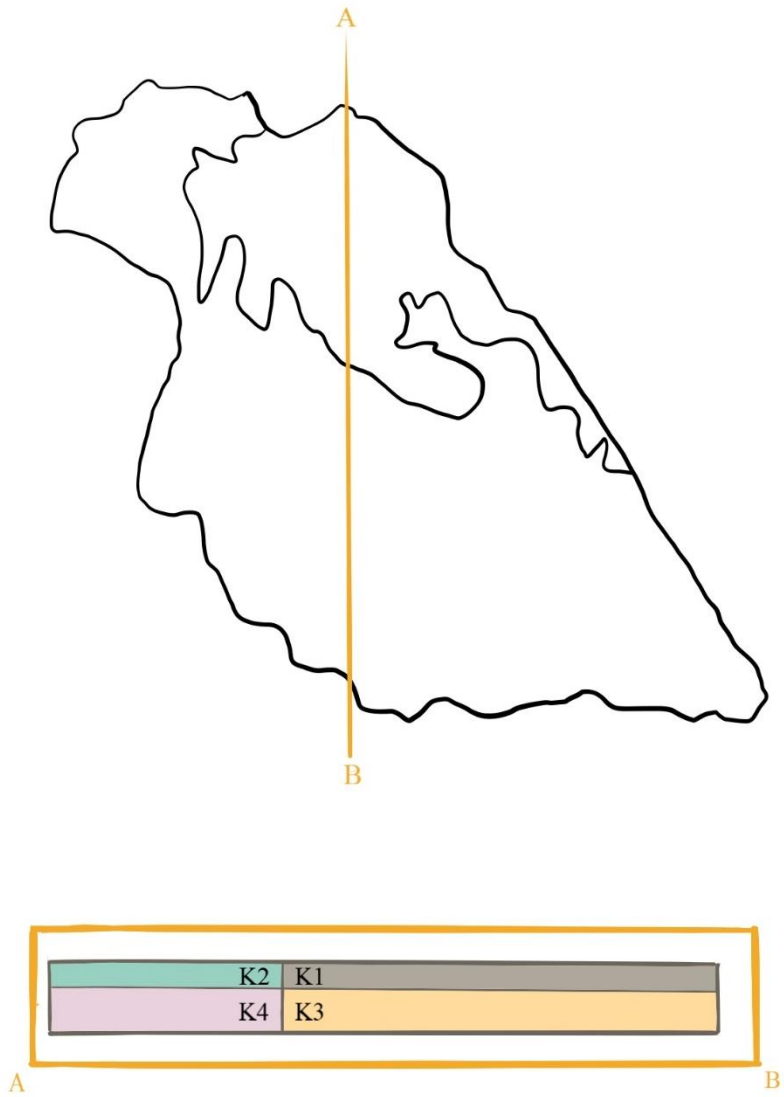

Figure 16: *Scheme showing the separation into hydraulic conductivity zones, where K1 and K2 are describing the upper layer, and K3 and K4 are describing the lower layer.*

Table 2: *Result of K values after the calibration of the steady state model.*

Zone	K- value (m/d)
K1	80
K2	0.00048
K3	50
K4	90

- *Specific yield and specific storage*

The storage coefficient was not relevant for the steady state model, but then used later in the transient model. It was calibrated for, together with the other parameter Evapotranspiration (ET), however, values were kept close to those found in literature. Values were assigned to zones S1, S2, S3 and S4 corresponding to the zones K1, K2, K3, K4, respectively, shown in **Figure 16**. The specific yield is the ratio between the volume of water that saturated soil or rock can yield by gravity, and the volume of the soil/ rock (Rasmussen, 1977). Thus, specific yield is usually lower for a clay layer and higher for a sandy layer. It can take months until gravity drainage will occur. The specific yield of the confining layer/ aquitard was only available in Erban and Gorelicks (2016) study and gave a value of $5*10^{-3}$. For the aquifer, Roberts (1998) suggested a value of 0.004 as mean from pumping tests in Prey Veng and Svay Rieng, which is typical for a thick confined sand and gravel aquifer. Erban and Gorelick presented a range of 0.05 to 0.2 for the specific yield of the aquifer. IDE (2009) presented the values $1*10^{-5}$ and $5*10^{-5}$ for different recharge scenarios, after calibration. It was not realistic to have lower specific yield values for the aquifer than for the aquitard, thus, Erban and Gorelick's values were adopted instead of using the ones from IDE.

The specific storage also needed to be determined for the transient model. It describes the volume of groundwater that an aquifer will absorb or expel when there is an increase or decrease of the pressure head by one unit amount (Fetter, 2001). In opposite to specific yield, a clay layer would have a higher value than a sandy layer.

After calibration the storage coefficient values resulted as presented in **Table 3:** Values of the specific yield and specific storage for the different zones. Zone distribution is set according to **Figure 16**., kept close to what was found in literature.

Table 3: *Values of the specific yield and specific storage for the different zones. Zone distribution is set according to* ***Figure 16****.*

Zone	Specific yield	Specific storage
S1	0.005	0.0002
S2	0.05	0.00002
S3	0.05	0.00002
S4	0.05	0.00002

3.3.3 Geologic layer elevations

Data on the layer elevations was taken from borehole logs including geology and stratigraphy of the PRASAC wells, which were shared by Michael Roberts. The logged wells, however, do not necessarily reach the bottom of the aquifer. Erban and Gorelick assumed the aquifer bottom to not exceed 100 m depth below msl, corresponding to the deepest logs. This is more than the depth that the wells in this part of Cambodia reach. The same strategy was adopted for this study, basing the bottom of the aquifer on the stratigraphic logs of the PRASAC wells. The points were then interpolated into a continuous bedrock layer using Empirical Bayesian Kriging, a straightforward method for interpolation, accounting for the error by doing repeated simulations to estimate the underlying semi variogram (Esri, 2012). The same interpolation method was used for interpolating the top surfaces of the old and young alluvium. **Figure 17**, **Figure 18**, and **Figure 19:** show the interpolated layer surfaces which were later used as input tif- file to the GMS MODFLOW model.

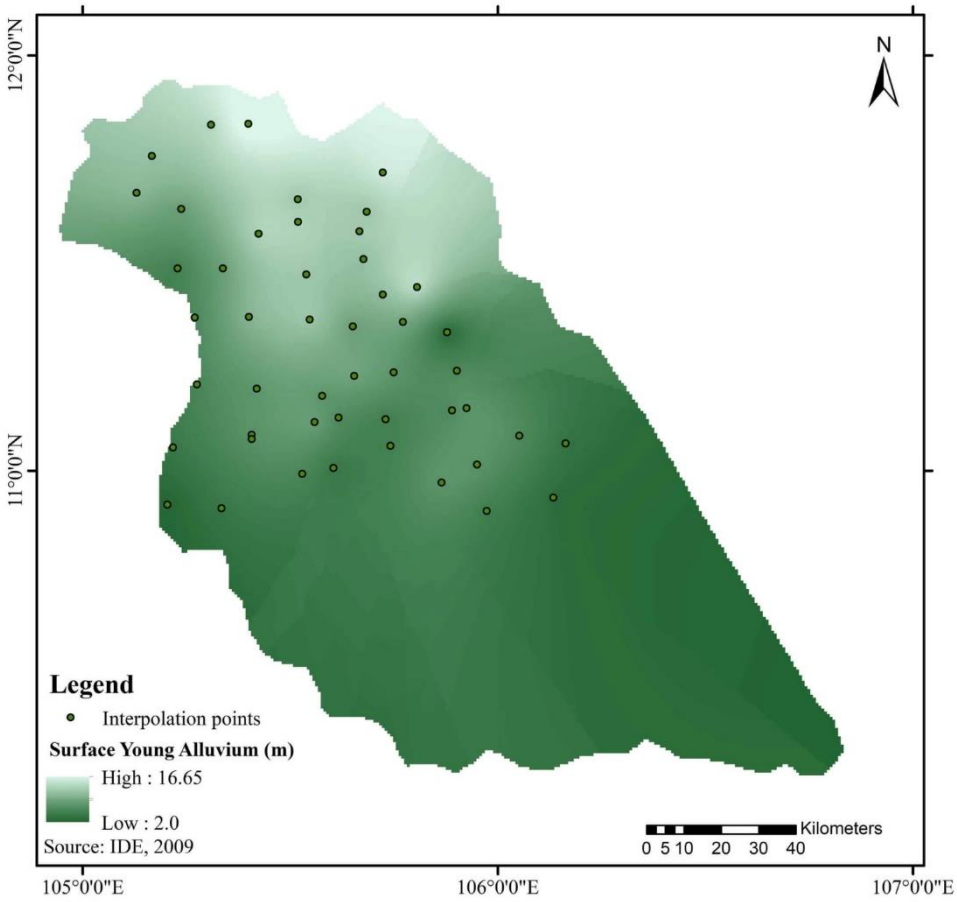

Figure 17: *Interpolated surface of the upper young alluvium layer of the model area.*

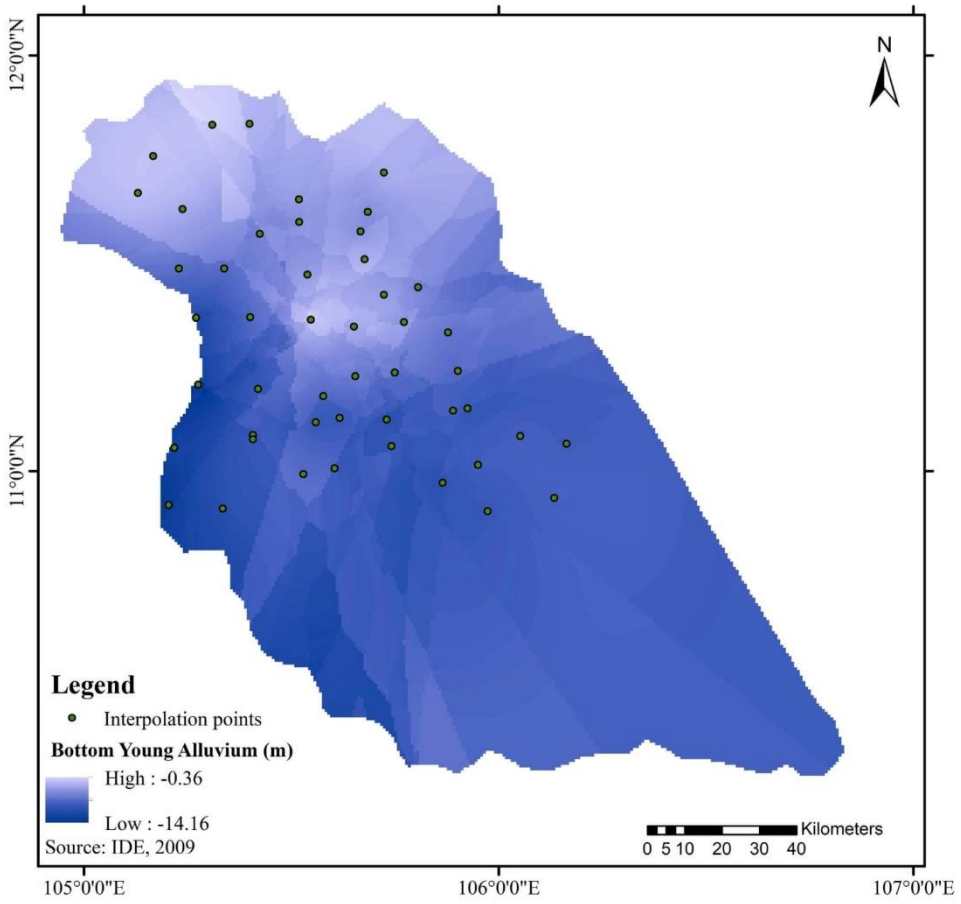

Figure 18: *Interpolated surface of the bottom of the young alluvium, and at the same time surface of the lower old alluvium layer.*

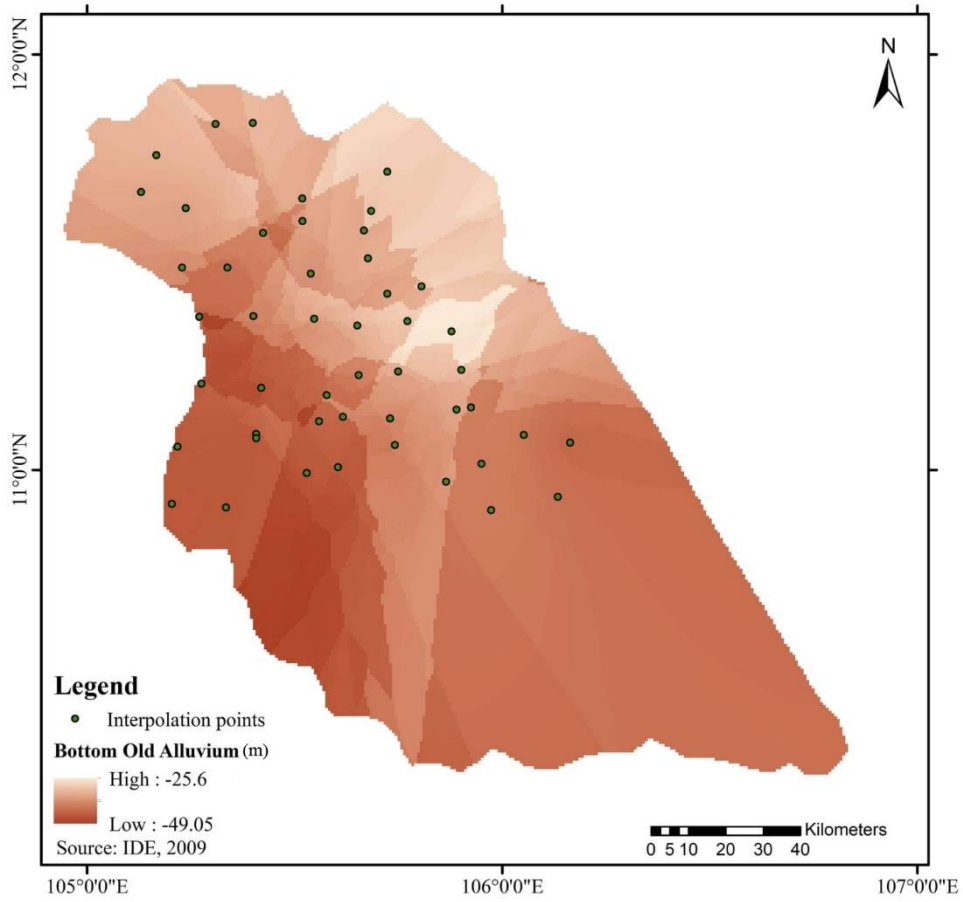

Figure 19: *Interpolation of the bottom of the old alluvium layer for the extent of the study area.*

3.3.4 River

The Mekong River determined the boundary conditions as described in section 3.3.1 and shown in **Figure 15.** There are several gauge stations measuring the daily river head along the Mekong River (**Figure 20**). In the steady state model, the river had a constant value at each gauge station, determined by taking the average of the daily values from March 2006 representing steady state conditions. The heads were adjusted slightly during the calibration of the steady state model. In the transient state model continuous monthly head data was assigned according to daily gauge measurements at the gauge stations along the Mekong River. The daily measurements were available for the complete time period (except at Chroy Chang Var measurements ended in

2012), more information on the gauge stations can be found in **Appendix 7**. The monthly means were computed from the daily measurements and inserted to the MODFLOW transient model.

Figure 20: *Scheme of the location of gauge stations and their name along Mekong River and the model boundary, where daily water levels were measured. (Source: MRC, 2022)*

3.3.5 Observation wells (records of groundwater level)

Groundwater observations over the past years are of high relevance for the study because the calibration requires a few years of regular head measurements. Water in the old alluvium aquifer is held under pressure by the overlaying young alluvium layer. Hence, when drilling boreholes through the young alluvium into the old alluvium, then the water level rises in the borehole until a few meters under the ground surface (IDE, 2009).

The European Union carried out a programme called "Programme de Réhabilitation et d'Appui au Secteur Agricole du Cambodge"(PRASAC) in Prey Veng and Svay Rieng province, in accordance to which a groundwater monitoring project with 49 observation wells throughout the two provinces was established in 1996 (IDE, 2009). Since then, groundwater levels were

collected and are still collected every month from the PRASAC wells, by the Provincial Departments of Water Resources and Meteorology (PDoWRAM). Some wells show a lack of data for a several months. Datasets for the PRASAC wells were provided from IWMI for the time period from 1996 to 2008 and for the years 2015 and 2016 for both provinces, however these datasets are lacking several months of data. IDE (2009) mentions that correction of the data, such as the subtraction of the height between ground surface and well casing height was made on-site, but is not recorded, leading to uncertainty whether the height of the apron is included or not and whether there is a set correction standard for each well or whether it is re- measured every time.
As further described in Chapter, up-to-date groundwater level data was collected by a field visit in Prey Veng and Svay Rieng, measuring the prevalent groundwater levels from the PRASAC observation wells. Several wells were not available for measurements, due to recent filling or utilization with pumping. Measurements were made for 17 observation wells in Prey Veng and 8 wells in Svay Rieng. Historical data on groundwater levels was requested from the Department of Water Resources and Meteorology. Provided upon request was data from 2015 to 2021 for 18 stations by the PDoWRAM in Prey Veng and data from 2015 to 2021 for 12 stations by the PDoWRAM in Svay Rieng.
The measurements made at the PRASAC wells, are depth to groundwater measurements. For the groundwater modelling part, these measurements were subtracted from the ground elevation to receive groundwater elevations. Since the ground surface was interpolated from the top young alluvium layer for the 49 monitoring wells, these values were used for the subtraction to receive the groundwater elevation.

The received groundwater files included several data lacks. A big lack was seen between January 2009 until December 2014, which could not be fixed by interpolation. Hence, the period from April 1996 to January 2009 was used for calibration and the period from January 2009 to March 2022 was used for validation purposes. Also, within those periods smaller data lacks were seen. It was important to have continuous data for the calibration period, thus, interpolation techniques were applied to fill the missing values during the calibration period. When one station was missing a few months of data, but neighbouring station data was available, then the correlation function between the data series of the two stations was used to determine the missing data period. When data of one month was not available for neighbouring or all

stations, then the average of the same month one year before and one year after was taken to determine the value for the missing month. **Figure 21** shows the measurements of depth of groundwater level to the surface in blue and the interpolated values in orange.

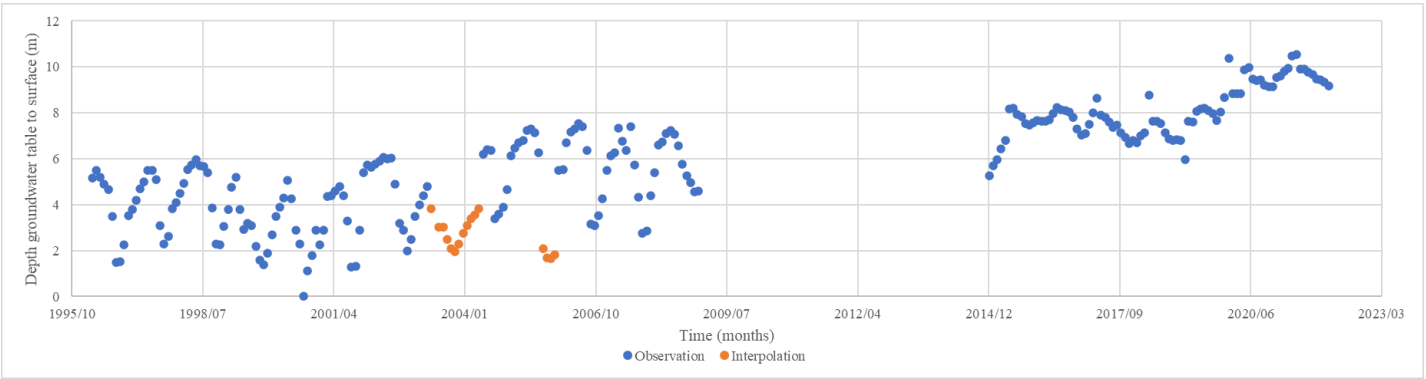

Figure 21: *Observations of depth of groundwater level to surface over time, available data from April 1996 to March 2022. The interpolated values of the data lacks during the calibration period are shown in orange.*

3.3.6 Vertical recharge (rainfall)

Vertical recharge was accounted for in the steady state model. In the transient state model vertical recharge was assigned for the northern aquifer part where the old alluvium reaches the surface, and where there is no confining layer preventing the aquifer from recharging.

Erban and Gorelick (2016) divert the modelled area into flooding and non-flooding zones, referring to the annual flooding extent according to a study by Marchland (2006). Constant rates were expected for the wet season recharge and the dry season ET within each zone and month. The flooding zone was expected to have more ET than recharge, thus, a yearly water loss of about 8 mm/year, and the non-flooding zone was assumed to have more recharge than ET, thus, a water gain of about 5mm/year. The extents of the two zones differ and hence, the average was a gain of 0.5 mm /year for the whole model. IDE used the same distribution as for their distribution of hydraulic conductivity. Since this study also based the zones on the Old Alluvium approaching the surface (slightly different from flood zones in Erban and Gorelick), it was done in accordance with IDE in this study, basing the spatial horizontal separation of the recharge zone on the Old Alluvium reaching the surface (**Figure 22**). Recharge was only modelled for the upper layer. Hence, created were two zones: one, where the confining Young Alluvium layer is covering the aquifer and no recharge to the underlying aquifer is possible and the second zone in the north- east, where the Old Alluvium reaches the surface and recharge from rain is possible. Recharge values differ, when looking at literature references: Values vary from 3- 20 mm/year (Erban and Gorelick, 2016; IDE, 2009) to 150 mm/ year (Rasmussen, 1977) to 450 mm/year (Kogyo, 2002).

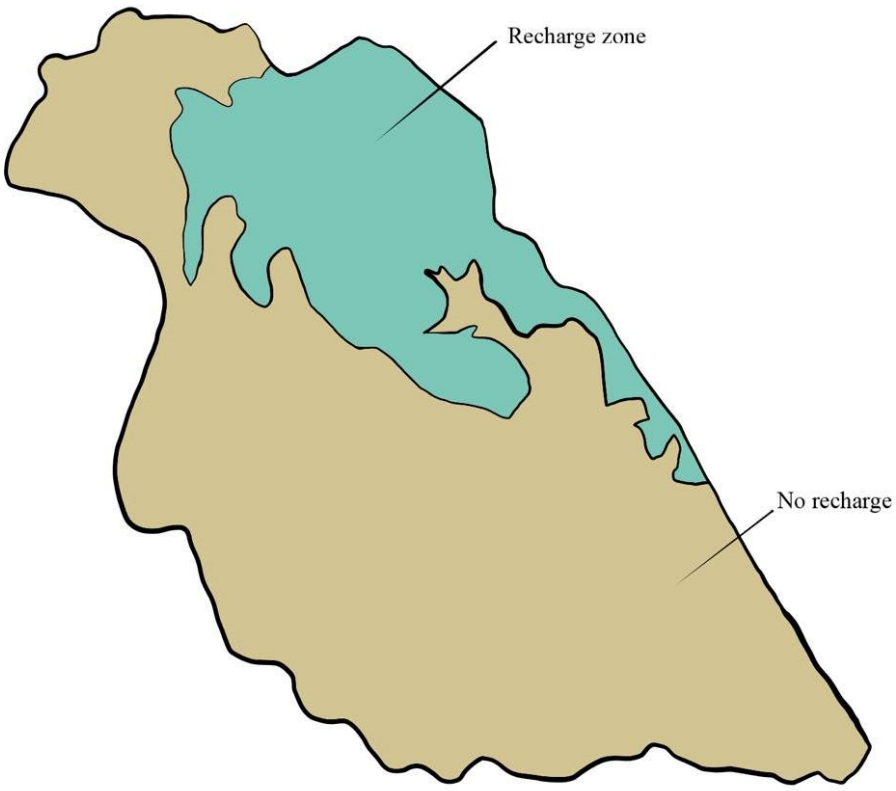

Figure 22: *Scheme of recharge and no- recharge zones within the model boundaries.*

The uniform recharge rate was directly correlated to the hydraulic conductivity, and both values were found after performing a sensitivity analysis and during calibration of the steady state model. The steady state recharge rate was kept close to literature values: IDE used two different scenarios, one using 15mm /year and one using 3mm/year. Thus, in this study the values were calibrated to lay within this range between 3 and 15 mm/year, also corresponding to Erban and Gorelick´s values. Resulting recharge values after the calibration of the steady state model are shown in **Table 4:** Recharge rates for the two modelled zones: Recharge zone and no recharge zone..

Table 4: *Recharge rates for the two modelled zones: Recharge zone and no recharge zone.*

Zone	Recharge rate (m/d)
Recharge zone	0.000016
No recharge zone	0

When setting up the transient model, it was necessary to distribute the recharge differently each month, according to amount of rainfall. The monthly recharge fractions were adopted from IDE (2009), seen in **Figure 23**. The Figure shows that September and October have the highest recharge, while December to April do not receive recharge at all. The fractions were then multiplied with the recharge rate that was computed from the steady state calibration and resulted in monthly values that were repeated for each year for the transient model for both, calibration and validation time period).
When running the transient model it was seen that there is too little water in the model. As the Mekong river and the vertical recharge through infiltration are the only two sources of water, and the Mekong had measured monthly water level, it was the most reasonable to increase the yearly recharge rate, and adjust the monthly values according to the fractions. The yearly recharge rate was adjusted to 80 mm/year (=0.00021913 m/d) (**Table 5**), laying in between the value suggested from Rasmussen (1977) and from Erban and Gorelick (2016). The model error estimates according to varying recharge rates are presented in the result chapter 4.2.1 Sensitivity analysis.

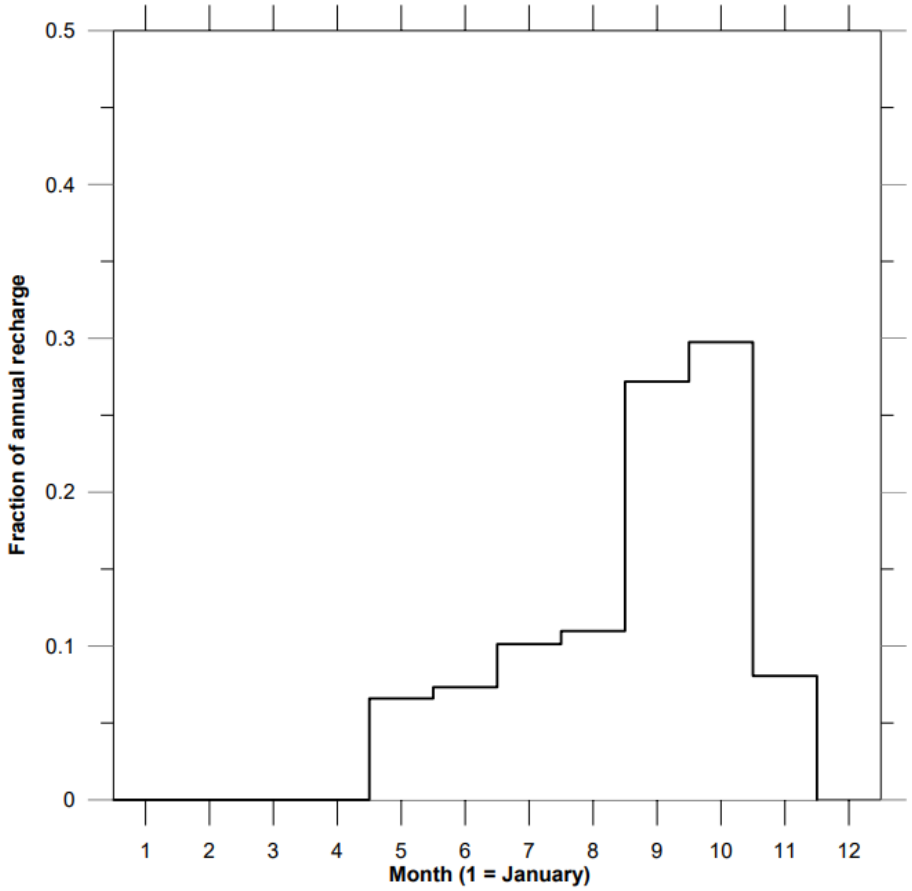

Figure 23: *Temporal distribution of recharge as a fraction of annual recharge (Source: IDE, 2009).*

Table 5: *Recharge fraction for each month, steady state rate and monthly varying recharge rate used for the transient model.*

Months	Recharge fraction	Steady state rate (m/d)	Recharge rate monthly varying (m/d)	
			before calibration	after calibration
1 (January)	0		0	0
2 (February)	0		0	0
3 (March)	0		0	0
4 (April)	0.065		0.00000104	0.0000142435
5 (May)	0.075		0.0000012	0.0000164348
6 (Juni)	0.1		0.0000016	0.000021913
7 (Juli)	0.11		0.00000176	0.0000241043
8 (August)	0.275		0.0000044	0.0000602608
9 (September)	0.295		0.00000472	0.0000646434
10 (October)	0.08		0.00000128	0.0000175304
11 (November)	0		0	0
12 (December)	0		0	0
SUM	1	0.000016	0.000016	0.00021913

3.3.7 Pumping for domestic usage

Pumping for domestic usage was not accounted for in the steady state model, since it is vertical movement of water.

For the transient model, the water that is extracted for domestic usage is relevant. In this study it was based on population estimates and estimations on daily water usage rate per person. In Prey Veng and Svay Rieng, 80 % of the people use groundwater in the household. **Figure 24** and **Figure 25** show the population estimates between 1998 and 2019 in Prey Veng and Svay Rieng, respectively. Estimations of the daily extraction rate were done for the different model time periods: For the calibration period (April 1996 to December 2005), population data from 1998 was chosen to be representative (**Table 6**). Data from 2005 was representative for the validation time period (2006-2008) (**Table 7**). For the pre- pandemic time between January 2015 and December 2019, the average of population values from 2013 and 2019 was taken (**Table 8**). The values from 2019 then represented the pandemic time between January

2020 and March 2022 (**Table 9**). The tables further show the calculated daily water usage rate for each time period, in the two provinces.

Population values were multiplied with the percentage of population using groundwater (2003 census data) (80 %) and with the average water use rate per capita based on rapid assessment in Svay Rieng/Prey Veng to receive an estimate of daily groundwater usage for domestic supply.
Since the location of extraction wells is unregulated and was unknown, it was not possible to directly add the pumping parameter to the MODFLOW model. Instead, it was subtracted from the evapotranspiration computations, as further described in the next Chapter Error! Reference source not found..

Table 6: *Calculations on estimates of daily groundwater extraction for domestic use in Prey Veng and Svay Rieng, approximated for the calibration period (April 1996 – December 2005) using population data from 1998. (Source: Source: seicdata.com, 2022)*

	Prey Veng	**Svay Rieng**
A) Population 1998 (Census data)	(a) 947500	(b) 480000
B) Percentage of population using groundwater (2003 census data)	80 %	80%
C) Average per capita water use based on rapid assessment in Svay Rieng	50 L/person/day	50 L/person/day
D) Daily groundwater extraction = ((A(a) + A(b)) x B/100 x C/1000	**57100 m^3/day**	

Table 7: *Calculations on estimates of daily groundwater extraction for domestic use in Prey Veng and Svay Rieng, approximated for the validation period (January 2006 – December 2008) using population data from 2005. (Source: Source: seicdata.com, 2022)*

	Prey Veng	**Svay Rieng**
A) Population 2005 (Census data)	(a) 945000	(b) 483000
B) Percentage of population using groundwater (2003 census data)	80 %	80%
C) Average per capita water use based on rapid assessment in Svay Rieng	50 L/person/day	50 L/person/day
D) Daily groundwater extraction = ((A(a) + A(b)) x B/100 x C/1000	**57000 m^3/day**	

Table 8: *Calculations on estimates of daily groundwater extraction for domestic use in Prey Veng and Svay Rieng, approximated for the pre-pandemic period (January 2015– December 2019) using population data from 2013 and 2019 (average). (Source: Source: seicdata.com, 2022)*

	Prey Veng	**Svay Rieng**
A) Population average 2013 and 2019 (Census data)	(a) 1110000	(b) 552000
B)Percentage of population using groundwater (2003 census data)	80 %	80%
C) Average per capita water use based on rapid assessment in Svay Rieng	50 L/person/day	50 L/person/day
D) Daily groundwater extraction = ((A(a) + A(b)) x B/100 x C/1000	**66500 m^3/day**	

Table 9: *Calculations on estimates of daily groundwater extraction for domestic use in Prey Veng and Svay Rieng, approximated for the pandemic time period (January 2020 – March 2022) using population data from 2019. (Source:seicdata.com, 2022)*

	Prey Veng	**Svay Rieng**
A) Population 2019 (Census data)	(a) 1058000	(b) 525500
B)Percentage of population using groundwater (2003 census data)	80 %	80%
C) Average per capita water use based on rapid assessment in Svay Rieng	50 L/person/day	50 L/person/day
D) Daily groundwater extraction = ((A(a) + A(b)) x B/100 x C/1000	**63340 m^3/day**	

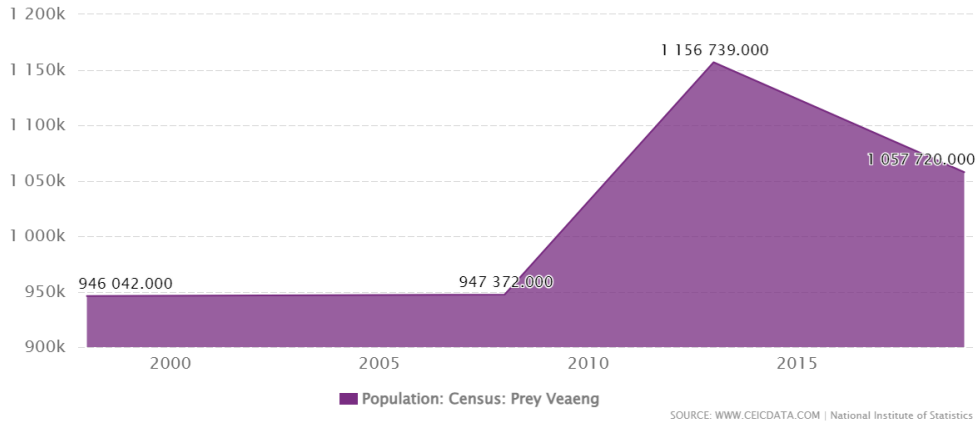

Figure 24: *Population in Prey Veng, 1998 to 2019. (Source: Source: seicdata.com, 2022)*

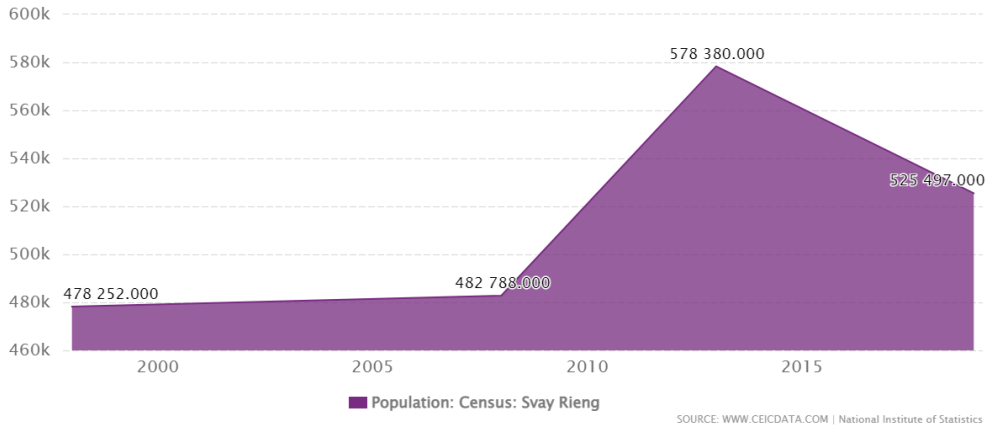

Figure 25: *Population in Prey Veng, 1998 to 2019. (Source: Source: seicdata.com, 2022)*

3.3.8 Evapotranspiration

ET was included only in the transient state model, by activating the Evapotranspiration Segments Package (ETS) package. The ETS package allows to add values for each defined stress period, meaning for each modelled month in this model. Parameter values to specify within the package are the maximum ET rate, an ET surface elevation and an ET extinction depth which is relative to the ET surface elevation. **Figure 26Error! Reference source not**

found. visualizes the different parameters that are to be specified in the ETS package.

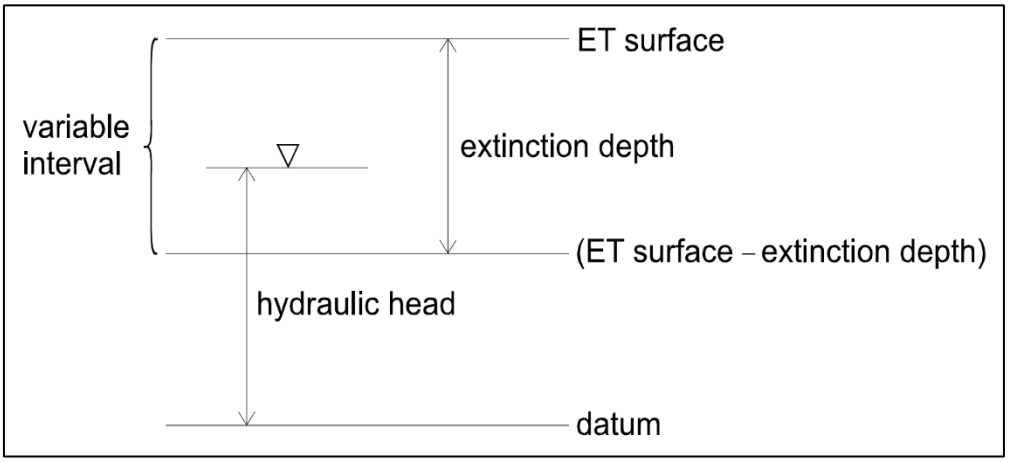

Figure 26: *Parameters of the ETS package to be defined in the transient model. (Source: Aquaveo, 2022)*

If the water table is above the ET surface elevation, then ET happens at its specified maximum rate. When the water table lays below the extinction depth, then there is no ET taking place. If the water table lays within the ET surface elevation and the extinction depth, then ET is dropping linearly, being at maximum at the ET surface and at 0 at the extinction depth. With the ETS package it is possible to further define the relationship of ET rate and the hydraulic for the heads between ET surface and the extinction depth to be non-linear. This can be done by specifying segments that describe the relationship between ET rate and the hydraulic head, as seen in**Figure 27**. In this model the relationship was assumed to have linear conditions.

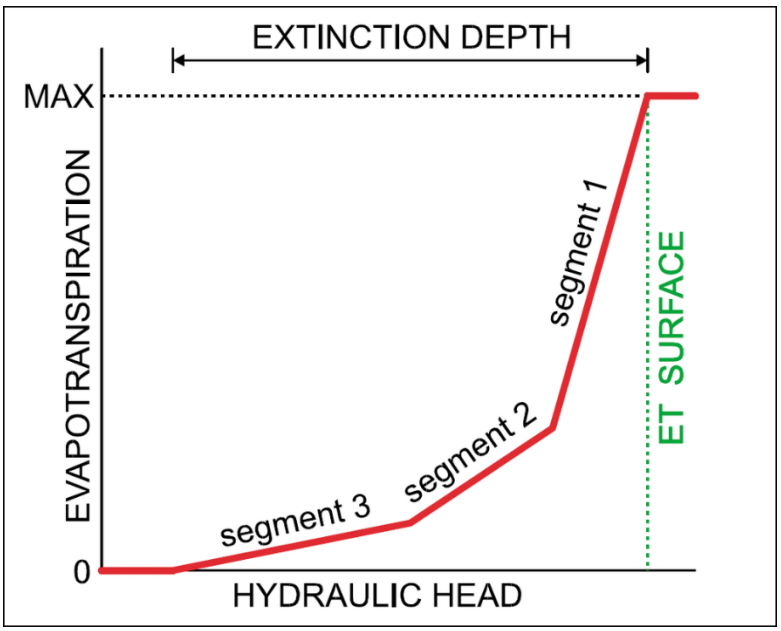

Figure 27: *Relationship between ET and hydraulic head, specified by segments in the ETS package. (Source: Aquaveo, 2022)*

ET was calibrated with transient conditions, and it affected only the upper aquifer layer. The model area was separated into two zones. Since the area of focus was Prey Veng and Svay Rieng, where most of the area is used for agriculture (**Figure 3**), the border between Cambodia (Prey Veng/Svay Rieng) and Vietnam was used to separate the two ET zones, as shown in **Figure 28**. While the ET zone 2, corresponding to the area of Vietnam, had constant values for the ET rate to be solved for using PEST, the algorithm was set up to solve for an ET rate varying with the monthly time steps in Zone 1 (Prey Veng, Svay Rieng). ET extinction depth and ET surface were both kept to a constant throughout the respective time period that was used for computation. The objective was that ET computations could then be compared with the remote sensing results, when running the model for the pandemic years (2019- early 2022). Furthermore, the pre- pandemic results could be compared to the results from pandemic years. The calibration process for the transient model is further described in Chapter **3.5** Calibration

ET was purely established from calibration using parameter estimation by setting a reasonable min and max for the automated calibration. The aim of the calibration was thereby to have the computed water levels laying close to the

measured water levels at the observation wells. Since ET was the only missing parameter, it was calibrated to fulfil this aim. Assuring realistic values was done by setting minimum and maximum value for extinction depth, ET surface and ET rate. Thus, ET acts as a factor balancing the model for optimal calibration without taking physical processes of ET, such as soil type or climate into account. Therefore, it could be assumed that groundwater pumped for domestic use is included within the ET parameter, since it was not possible to directly add it to the model. After computing ET, the estimates of domestic groundwater usage were subtracted from the ET results, assuring that ET can give an estimate on water usage for irrigation.

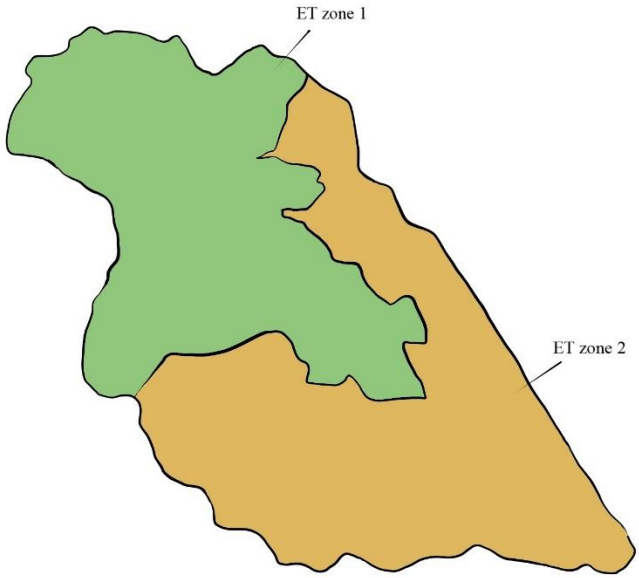

Figure 28: *Scheme of ET zone 1 and ET zone 2 within the model boundaries.*

3.4 Sensitivity Analysis

A sensitivity analysis for the steady state model was performed while calibrating, meaning the determination of how sensitive the model is to changes of certain parameters. This was helpful to find the optimal value for the best model output during and it can also help to determine the parameters that do not affect the model outcome when changing the value within the reasonable range. It was looked at the hydraulic conductivity for the four zones (K1, K2, K3 and K4 (**Figure 16**)), and at the recharge parameter (**Figure 22**).

The sensitivity analysis was based on three statistical indices: The mean error (ME) estimates the average between the differences between computed and observed values (Statistics How To, 2016). The Mean Absolute Error (MAE) measures the mean between the absolute differences between measured and computed values, without assigning a weight. The Root Mean Square Error (RMSE) takes the square root of the average of the squared differences between measured and computed values, thereby estimating the average magnitude of the error (Medium, 2016).

A sensitivity analysis was also carried out for the transient model, looking at specific storage, specific yield, and recharge. Results are presented in section **4.2.1** Sensitivity analysis

3.5 Calibration

The steady state model was calibrated for hydraulic conductivity and recharge, and the transient model was calibrated for mainly ET and recharge, but also specific storage and storage coefficients were slightly adjusted, though kept close to literature values. For calibration, the observation head interval was set to 1.5, representing the estimated error (+ or -) in the observed value and is representing the calibration target. This means, if the model output is resulting in a computed water level laying within an interval of +- 1.5 m from the observed value, calibration is achieved for the observation well. Reaching calibration is represented by green coloured bars at the respective observation well, after running the model. Yellow coloured bars refer to values laying outside the target (1.5) but are lower than the interval of +/- 3 from the observed value. Red coloured bars refer to values outside of the interval of +/- 3 from the observed value. The observation head confidence was set to 95%, representing the confidence in the error estimation. During calibration the values of different coverages were adjusted in order to achieve computed head

values at the observation wells that lie within the observation head interval of +/- 1.5 m. Most important were the observations closer to the centre of Prey Veng and Svay Rieng. The input variables were described earlier in Chapter 3.3 Data inputs. The steady state calibration constant values were used as described earlier.
The transient model was calibrated with monthly data for the groundwater levels, from the period April 1996 to December 2005. The sensitivity analysis was helpful to determine the most suitable values for the best model performance.
Calibrating the transient model was done by firstly adjusting the specific yield and specific storage parameter, however, keeping it close to literature values. Secondly, recharge was adjusted according to outcomes of the sensitivity analysis. As stated earlier it was chosen to continue with a yearly recharge of 80 mm/ yr, distributed over the months, according to the monthly fractions that were presented in **Table 5**. It was taken into account that the model needed about two years for warming up. Focus was set on the years after the two year warm up for calibration.

Furthermore, the ET parameter had to be calibrated and this was done by applying the powerful, non-linear parameter estimation algorithm called PEST (Parameter ESTimation), which was developed by John Doherty of Watermark Computing and is available within the GMS MODFLOW software. This algorithm applies automated parameter estimation, also known as inverse modelling, adjusting certain input parameters within the algorithm run to receive the best match between observed and calibrated values. It was possible to also specify solver parameters, such as the number of total optimization iterations, or the number of iterations with no improvement, after which the model would end to converge, when no improvement was made during the previous three iterations.

Since ET was calibrated and inserted to the model via the ETS package, there were three variables to be calibrated for: ETS rate, ETS surface and ETS extinction depths, as introduced in Chapter **Error! Reference source not found.**. Minimum and maximum value for each of the variables could be specified in order to keep the values within a reasonable range. Due to difficulties and error conditions when running PEST for calibration, the model was built up a second time starting from the working steady-state model, however, experiencing similar issues as before.

Table 10 shows the minimum and maximum for each of the variables. ETS surface was kept constant for each timestep, using the minimum and maximum of the top surface elevation of the upper layer. Research gave that ETS extinction depth can be represented by root depths (FAU College of Engineering, 2022). Rice roots are very shallow, and that is why the minimum was set to 0.2. The maximum was set to 2, according to values used in a MODFLOW tutorial. The annual ET rate in Cambodia is about 1300 mm/year (ADB, 2019). Since ET was representing GW extraction, values were set to have a quite wide range between 0.0001 and 10 m/d.

Due to difficulties and error conditions when running PEST for calibration, the model was built up a second time starting from the working steady-state model, however, experiencing similar issues as before.

Table 10: *Minimum- maximum range for ETS rate, ETS surface and ETS extinction depth for the ET parameter estimation according to PEST algorithm. Parameters were assigned for both zones, though ETS rate in the ET zone 1 had transient conditions, while it was constant for the ET Zone 2.*

	ET	
	Minimum	**Maximum**
ETS rate (m/d)	0.0001	10
ETS surface	2	17
ETS extinction depth	0.2	2

3.6 Validation

The period for validation of the transient model was chosen to be from January 2005 to December 2008. Planned to be compared were the computed values for this period with the observed values at the observation wells, in order to validate the calibrated data for a new time period. Planned to be used for the validation was RMSE, MAE and ME as statistical indices, and visual graph comparison of the computed and observed water level.

3.7 Effect of irrigation changes on groundwater levels

The effect of irrigation changes on groundwater levels was examined by assuming a correlation between ET and groundwater amount used for irrigation during the dry season. As stated earlier, the groundwater model was solved for ET, which could give an indication on groundwater being used for irrigation after subtracting the amount that was approximated to be used for domestic supply. The model was then planned to run for the time period

January 2015 to December 2019 to represent the pre- covid conditions and from January 2020 to March 2022, to represent the pandemic time period.
Furthermore, the collected data on groundwater levels was analysed over the available time ranges (April 1996 – December 2008 and January 2015-December 2022). Yearly decline of the groundwater level was computed for certain randomly chosen wells, P01, P05, P14, P21, P26, S10 and S18 and specified for each time period (calibration time period, validation time period, pre-covid time period and covid time period) in order to be able to make comparisons.

4. Results

4.1 Steady- state model

4.1.1 Sensitivity Analysis

In order to find a good calibration, a sensitivity analysis was carried out for the parameter's hydraulic conductivity and recharge. Error estimates ME, MAE and RMSE and used for comparison of different values. The range of values used for sensitivity analysis is reflecting the value range that was found in literature review.

Figure 29: Sensitivity analysis of K1 with Simulation 1 (K1= 0.00048 m/d), Simulation 2 (K1=0.0048 m/d), Simulation 3 (K1=0.048 m/d), Simulation 4 (K1=0.48 m/d) and Simulation 5 (K1= 1 m/d). shows no difference when changing K1 within the appropriate ranges, thus it is not a parameter influencing calibration.

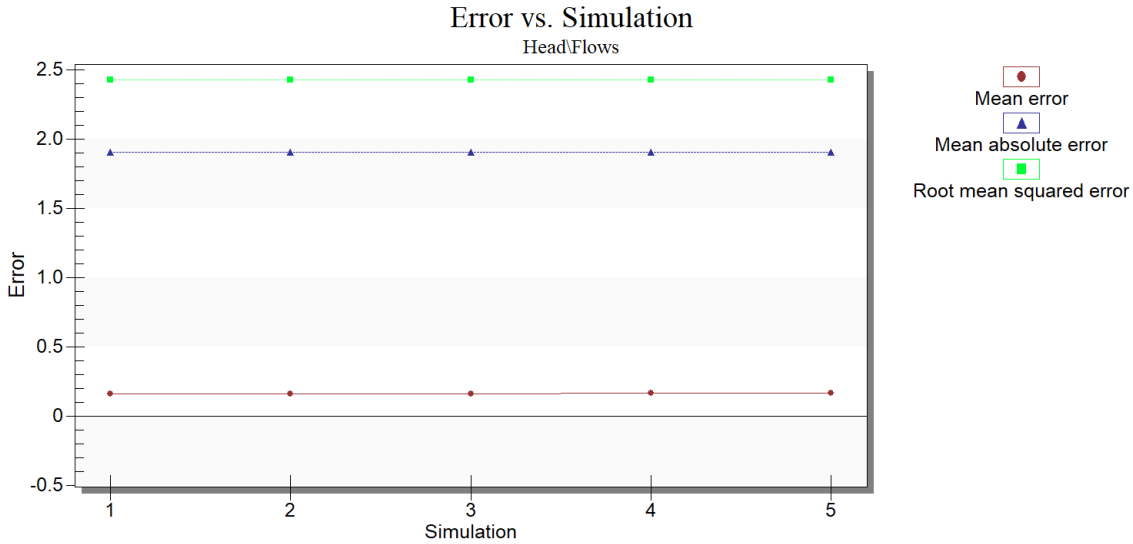

Figure 29: *Sensitivity analysis of K1 with Simulation 1 (K1= 0.00048 m/d), Simulation 2 (K1=0.0048 m/d), Simulation 3 (K1=0.048 m/d), Simulation 4 (K1=0.48 m/d) and Simulation 5 (K1= 1 m/d).*

Regarding K2, MAE and RMSE do not show large differences, however, ME does vary when increasing the value. **Figure 30:** Sensitivity analysis of K2 with Simulation 1 (K2= 30 m/d), Simulation 2 (K2=40 m/d), Simulation 3 (K2=50 m/d), Simulation 4 (K2=60 m/d) and Simulation 5 (K2= 70 m/d) and

Simulation 6 (K2= 80 m/d). shows that, according to ME, the optimal value lays between Simulation 3 (K2=50 m/d) and Simulation 4 (K2=60 m/d) with an ME of 0.

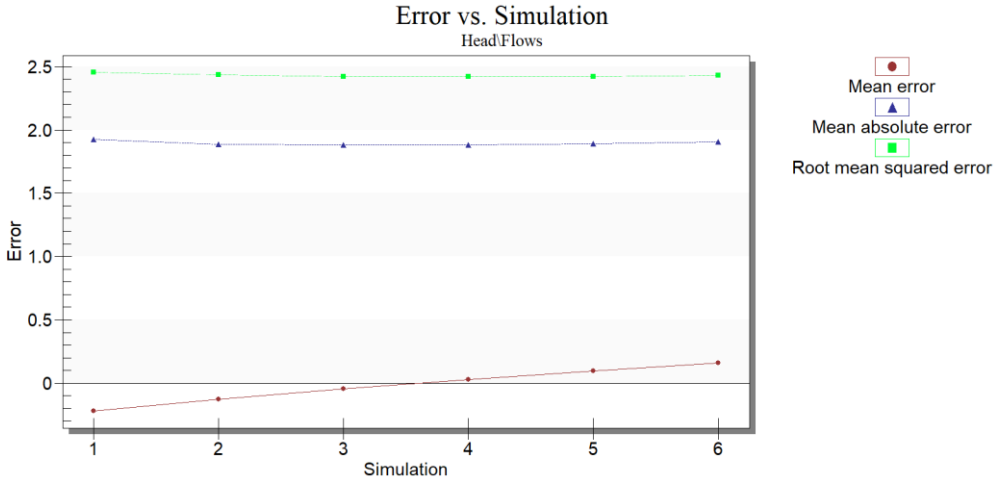

Figure 30: *Sensitivity analysis of K2 with Simulation 1 (K2= 30 m/d), Simulation 2 (K2=40 m/d), Simulation 3 (K2=50 m/d), Simulation 4 (K2=60 m/d) and Simulation 5 (K2= 70 m/d) and Simulation 6 (K2= 80 m/d).*

The sensitivity analysis of K3 shows variation in ME, MAE and RMSE, as shown in **Figure 31**: Sensitivity analysis of K3 with Simulation 1 (K3= 48 m/d), Simulation 2 (K3=70 m/d), Simulation 3 (K3=90 m/d), Simulation 4 (K3=110 m/d) and Simulation 5 (K3= 130 m/d) and Simulation 6 (K3= 150 m/d), Simulation 7 (K3= 170 m/d), Simulation 8 (K3= 190 m/d), Simulation 9 (K3= 210 m/d), Simulation 10 (K3= 230 m/d), Simulation 11 (K3= 250 m/d), Simulation 12 (K3= 270 m/d), Simulation 13 (K3= 280 m/d)., thus having effect on the calibration. All three error estimates are closest to 0 in between Simulation 2 (K3=70 m/d) and Simulation 3 (K3=90 m/d).

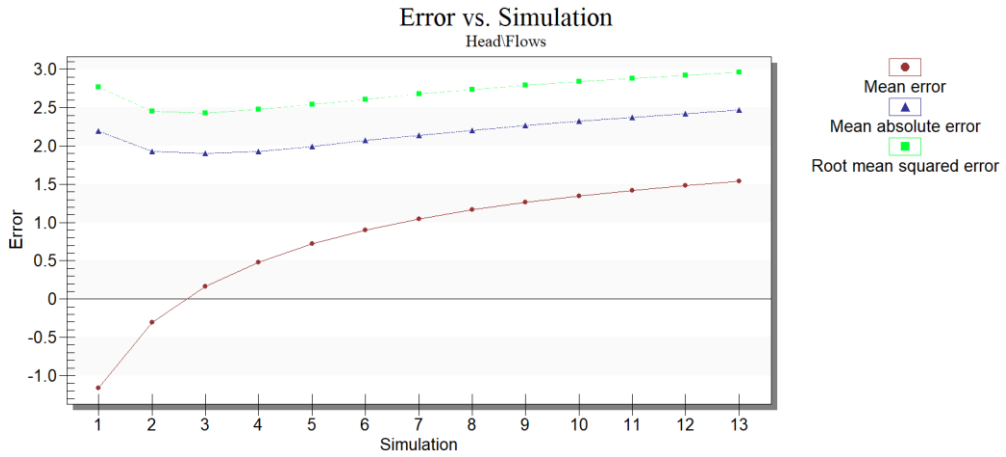

***Figure 31**: Sensitivity analysis of K3 with Simulation 1 (K3= 48 m/d), Simulation 2 (K3=70 m/d), Simulation 3 (K3=90 m/d), Simulation 4 (K3=110 m/d) and Simulation 5 (K3= 130 m/d) and Simulation 6 (K3= 150 m/d), Simulation 7 (K3= 170 m/d), Simulation 8 (K3= 190 m/d), Simulation 9 (K3= 210 m/d), Simulation 10 (K3= 230 m/d), Simulation 11 (K3= 250 m/d), Simulation 12 (K3= 270 m/d), Simulation 13 (K3= 280 m/d).*

Also changing K4 shows variations in all three error estimates. The point where all three of them are closest to 0 is between Simulation 6 (K4= 40 m/d) and Simulation 7 (K4= 50 m/d), as shown in **Figure 32**.

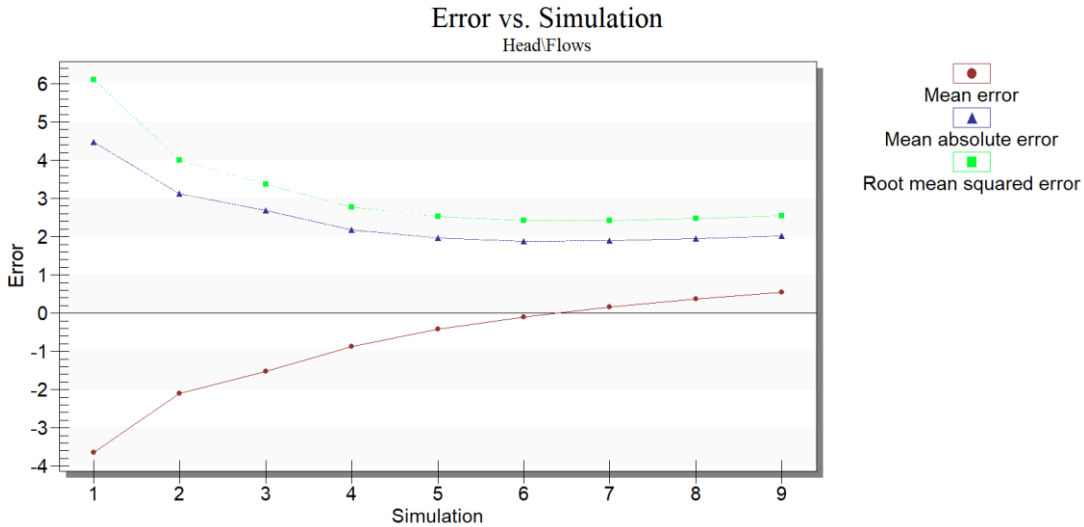

***Figure 32:** Sensitivity analysis of K4 with Simulation 1 (K4=1 m/d), Simulation 2 (K4=5 m/d), Simulation 3 (K4=10 m/d) and Simulation 4 (K4= 20 m/d) and Simulation 5 (K4= 30 m/d), Simulation 6 (K4= 40 m/d), Simulation 7 (K4= 50 m/d),), Simulation 8 (K4= 60 m/d) and Simulation 9 (K4= 70 m/d).*

Changing the recharge parameter within the suitable ranges, as described in Chapter 3.3.6 Vertical recharge (rainfall) shows effects on the magnitude of error. **Figure 33** shows that all three error estimates lay closest to 0 between Simulation 3 (Re=0.00001480 m/d) and Simulation 4 (Re=0.00001810 m/d). All parameters described above resulted in calibrated values being close to those found optimal when performing this sensitivity analysis.

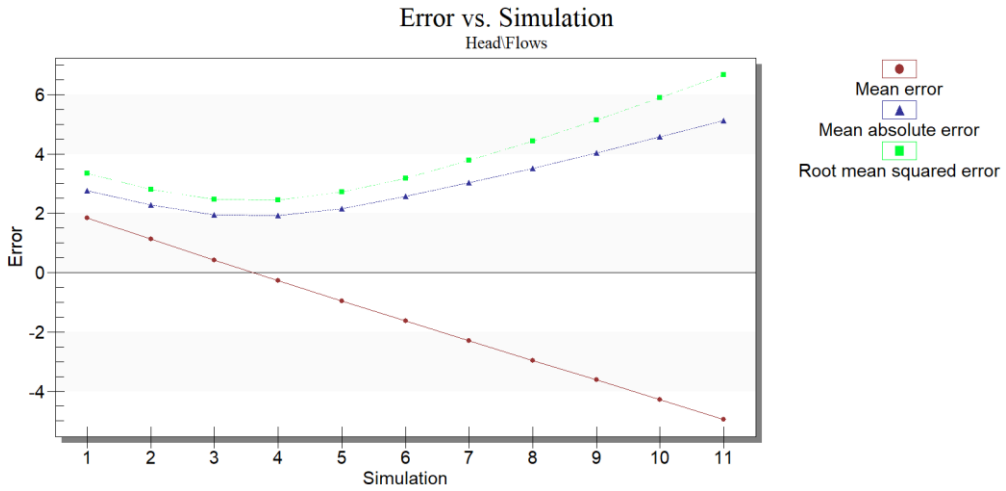

Figure 33: *Sensitivity analysis of the recharge parameter (Figure 22) with the following values applied in the recharge zone: Simulation 1 (Re= 0.00000822 m/d), Simulation 2 (Re= 0.00001150 m/d), Simulation 3 (Re=0.00001480 m/d), Simulation 4 (Re=0.00001810 m/d) and Simulation 5 (Re= 0.00002140 m/d) and Simulation 6 (Re= 0.00002470 m/d), Simulation 7 (Re= 0.000028 m/d), Simulation 8 (Re= 0.0000313 m/d), Simulation 9 (Re= 0.0000346 m/d), Simulation 10 (Re= 0.00003790 m/d) and Simulation 11 (Re= 0.0000412).*

4.1.2 Calibration results

The best result of the calibrated steady state model is pictured in **Figure 34**. Each observation well has an error bar, where most of the bars in the centrum of the model area are green, and some orange, mainly further in the south. Two bars are red meaning a computed water level that does not lay within the +- 3 m interval from the measured water level. The observation well with the red bar in the east, shows some flooding in the area around but the magnitude of flood is very low.

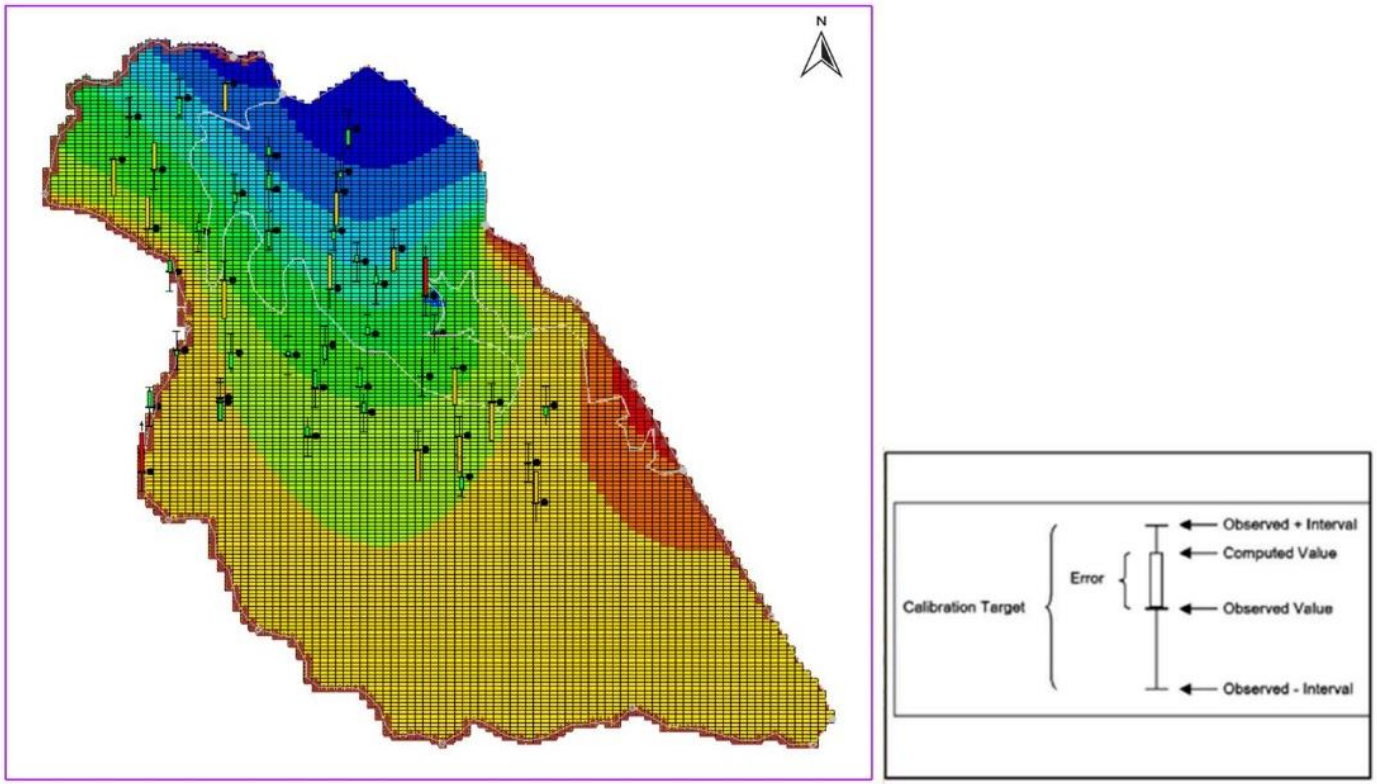

Figure 34: *Calibrated steady state model with error range of simulation wells. Green bars refer to values within the interval +/- 1.5, yellow bars refer to values laying outside the target (1.5) but are lower than the interval of +/- 3 from the observed value. Red bars refer to values outside of the interval of +/- 3 from the observed value.*

For the calibrated steady state model, Mean Residual of the head (ME) was 0.11, Mean Absolute Residual of the head (MAE) was 1.46 and Root Mean Squared Residual of the head (RMSE) was 1.86. Comparing those values to the ones that were produced during sensitivity analysis, shows that the MAE and RMSE values are closer to 0 after combining the optimal values that were found in the sensitivity analysis, into the calibrated model. **Figure 35** shows the correlation between computed and observed values of the steady state model. It is seen that the computed heads can be both, over and underestimated compared to the measured values. This explains the ME, taking the average of all positive and negative errors (residuals), being closer to 0 than the MAE, taking the average of the absolute errors.

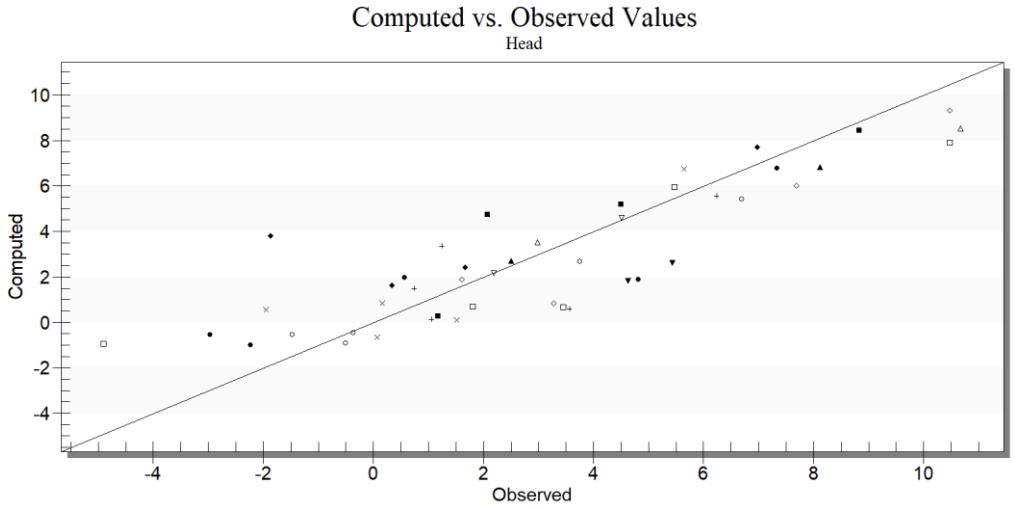

Figure 35: *Graph depicting computed vs. observed head values (m) of the steady state calibrated model.*

4.2 Transient state model

The visualizations of the first and second build up of the transient model are found in **Error! Reference source not found.** and **Error! Reference source not found.**.

4.2.1 Sensitivity analysis

The sensitivity analysis for specific storage and specific yield, gave no significant changes in between the values that were run for the sensitivity analysis. **Figure 36** shows the error estimates for different input values for

specific yields. The error estimates ME, MAE and RMSE do not vary significantly, the model is not very sensitive to small changes in specific yield. Also, the specific storage did not show changes when increasing or decreasing it within the realistic range. Hence, the values were kept close to those found in literature.

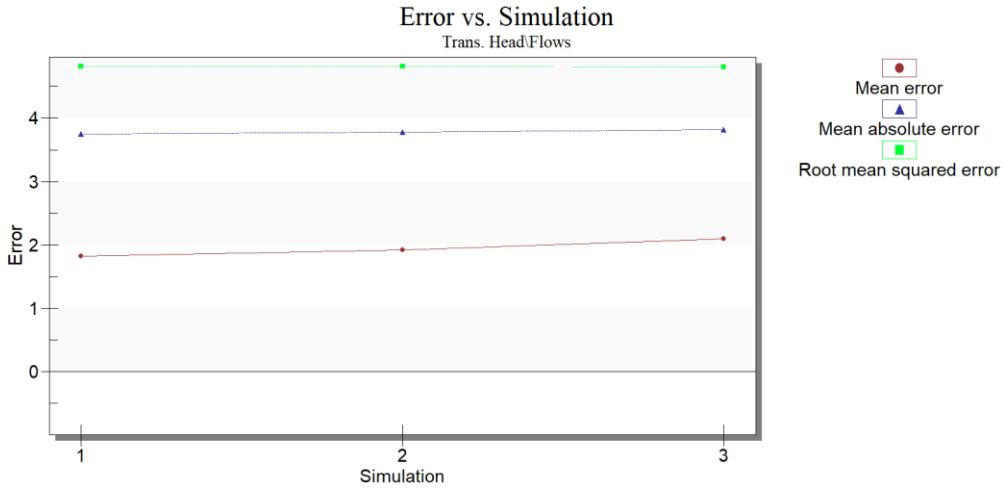

Figure 36: *ME (m), MAE (m) and RMSE (m) for different values for specific yield for the aquifer layer: Simulation 1 (specific yield = 0.05), Simulation 2 (specific yield = 0.1) and Simulation 3 (specific yield = 2.0).*

Regarding the recharge parameter, increasing the value showed an error decrease, as seen in **Figure 37**. When modelling an annual value of 70 m/d (Simulation 7) flooding started to occur at some small parts of the model (**Appendix 1**). This was considered to be acceptable, as ET was not yet applied to the model.

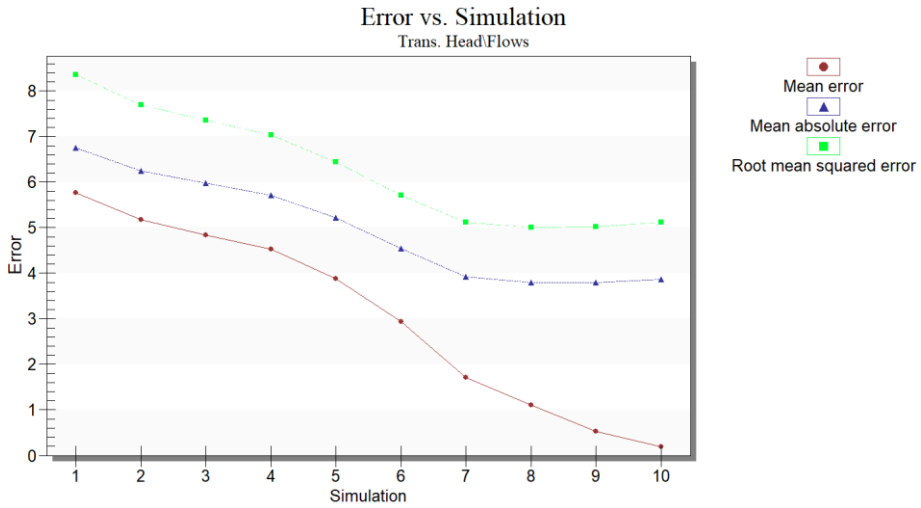

Figure 37: *Sensitivity analysis of recharge, with the following values applied in the recharge zone: Simulation 1 (Re= 0.0000016 m/d), Simulation 2 (Re=0.0000411 m/d = 15 mm/yr), Simulation 3 (Re=0.00005479m/d = 20 mm/yr), Simulation 4 (Re=0.00006848 m/d= 25mm/yr) and Simulation 5 (Re= 0.00009586 m/d = 35 mm/yr) and Simulation 6 (Re= 0.00013696 m/d = 50 mm/yr), Simulation 7 (Re= 0.00019175 m/d = 70 mm/yr), Simulation 8 (Re= 0.00021913 m/d = 80 mm/yr), Simulation 9 (Re= 0.00024654 m/d = 90 mm/yr) and Simulation 10 (Re= 0.00027392 m/d = 100 m/yr).*

4.2.2 Calibration

Calibrating recharge, specific storage and specific yield in accordance with the results from the sensitivity analysis, resulted in a decreased overall error, considering all time steps within the calibration time period, as it can be read from **Table 11**.

Table 11: *ME (m), MAE (m) and RMSE (m) of the transient model (all time steps) for the calibration period, before and after calibration.*

	before calibration	**after calibration**
ME	1.88	0.56
MAE	2.97	1.93
RMSE	3.63	2.55

The automated calibration of ET using PEST was a challenge. Errors were faced, when starting the run. Only one run was successful, however the computation took above 10 hours, and the result was not satisfactory. The algorithm had stopped after 3 iterations, as there was no significant improvement of the model outcome. It was seen that the other parameters were

optimized, however not the transient ET rate that was supposed to be varying at each time step for ET zone. After the PEST run, this transient ET was kept at starting values, even though it was specified to be a subject of calibration. Furthermore, ME, MAE and RMSE did not vary from the values before the PEST run. Making only the smallest changes in the parameter file that was running successfully, i.e., simplifying the parameters to be calibrated for, resulted in errors preventing the model from converging.

4.2.3 Parameter estimation

The automated calibration of ET using PEST was a challenge. Faced were errors when starting the run. Only one run was successful, however the computation took above 10 hours, and the result was not satisfactory: The algorithm had stopped after 3 iterations, as there was no significant improvement of the model outcome. It was noticed that the ET varying for each time step did not change. Other parameters were optimized, however not the transient ET rate that was supposed to be varying at each time step for ET zone. After the PEST run, this transient ET was kept at starting values, even though it was specified to be a subject of calibration. Furthermore, ME, MAE and RMSE did not vary from the values before the PEST run. Making only the smallest changes in the parameter file that was running successfully, i.e. simplifying the parameters to be calibrated for, resulted in errors preventing the model from converging.

Various efforts were made to try making PEST run. First of all, a Modflow support group was used to find help with PEST, however, there was a lack of response from the individuals. Instead, the model was built up again, starting from the steady state condition. Adding the transient data again, another error occurred: Cannot open the .hed file. This error occurred when adding transient groundwater level observation data. However, still unclear what resulted in this error, it was fixed when doing the process of adding transient data into the model another, third time. Consequently, a second, working transient model had been established.

After inserting the evapotranspiration variable and activating PEST, it did not converge at all this time but showed the error: Cannot find .par file. Trying to adjust other things such as deleting all saved recent model versions from the software and from the folder, or re- installing GMS Modflow, did not help.

4.2.4 Validation

The validation was supposed to be run using parameter estimation with PEST; however, the results during calibration were not satisfactory, and it could not yet be applied for validation.

4.2.5 Model analysis for pre-pandemic and pandemic time

The model was supposed to be solved for ET for the pre-pandemic and pandemic time period, estimating the evaporation and connecting it to the remote sensing study of irrigation. However, the parameter estimation with PEST during calibration was not satisfactory, and it could not be applied during the pre- and pandemic time.

4.3 Analysis of the collected groundwater level data

Firstly, the depth from surface to GW level for the different wells visited during the field visit in Cambodia in March 2022 are presented in **Table 12**. Orange marked values show the values that have exceeded the 6 m limit below which pumping is not possible anymore.

Table 12: *Surface to groundwater depth (m) measured during the field visit in Prey Veng and Svay Rieng. Orange marked values exceed the pumping limit of 6 m below surface, March 2022.*

Prey Veng	Depth (Surface to GW level)	Svay Rieng	Depth (Surface to GW level)
P01	12.14	**S06**	6.16
P03	14.49	**S10**	4.16
P04	10.03	**S11**	3.54
P05	12.97	**S12**	3.47
P06	5.9	**S13**	3.69
P07	6.22	**S17**	6.95
P08	3.12	**S18**	5.91
P09	3	**S20**	6.71
P14	10.1		
P15	11.35		
P19	7.73		
P21	7.45		
P22	8.43		
P23	8.64		
P24	7.98		
P25	0.26		

In **Figure 38** the yearly groundwater decline/increase is seen for a few randomly picked wells for each of the computational periods: Calibration time period, validation time period, pre-pandemic period, and pandemic period. It is seen that the values for pre-pandemic and pandemic time (after 2015) are higher than the ones from earlier days (1996 to 2008). Comparing only pre-pandemic and pandemic situations, it is seen that the decline is even more pronounced during the pandemic time. Seen is a strong decline in all presented wells, except P14, which shows a strong increase in groundwater level.

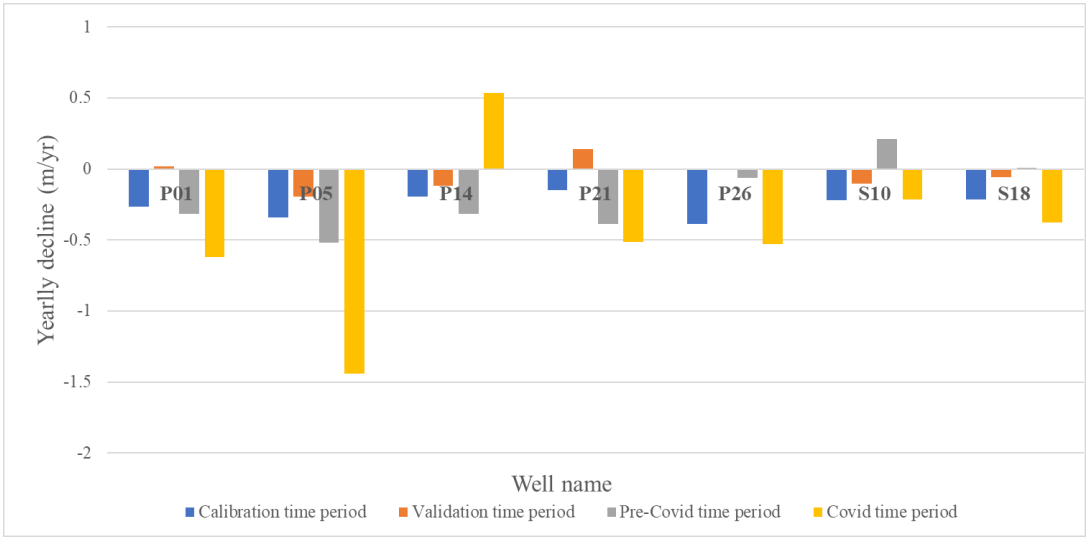

Figure 38: *Yearly groundwater decline of groundwater level (m/yr) for each of the computational periods: Calibration time period, validation time period, pre-pandemic period, and pandemic period.*

5. Discussion

This chapter will provide an interpretation of the model results, discusses the methodology, the limitation of the input parameters to the model and also gives an evaluation of the GMS MODFLOW software.

5.1 Interpretations of the model results

The sensitivity analysis of the steady state model showed that K2, K3, and K4 and the recharge parameter have the largest effect on the model outputs and proposed suitable values for a good calibration result. The steady state calibration was thus sufficient, showing many computed water levels being within 1.5 m from the measured value. Only computed values of two wells were laying outside of the 3 m interval from the measured value. The results of the sensitivity analysis of the transient model show that the model is not very sensitive to changes in specific yield and specific storage, thus, set to literature values, but therefore it shows a high sensitivity to the recharge parameter. Increasing the recharge could further decrease the error estimates. Calibrating the transient model without taking the pumping into account yet showed surprisingly good results, considering that this part of Cambodia experiences dry and wet season and the steady state model was only done for a specific time in the dry season in 2006. The good interaction looking at the different months after the model warm up period of a few years, shows that groundwater models are indeed able to give an estimate of the reality, even if reality is complicated.

PEST was, in the beginning, seen as a powerful tool to compute ET from the groundwater model and relate the outcome to changes that were earlier seen in the remote sensing analysis. However, the computational effort for PEST is high when using a transient model like in this study: PEST was sensitive to the smallest changes made in the parameter specifications, causing immediate error. Furthermore, a successful run took ten hours for only three iterations. If it was possible to have a satisfactory run using PEST, it would be expected to be running for many hours, if not even days.

Looking at the change in groundwater level only, an increased decline in most of the wells in the pandemic time, compared to 1996- 2005, 2005-2008 and 2015-2019 was shown, suggesting either an increased use of the water for irrigation and households, or climatic changes. Furthermore, **Table 12** showed that most wells already experience water levels below the pumping limit of 6

m, which is an alarming sign that measures to control groundwater usage need to be taken immediately. The immediate consequence will be that water cannot be pumped for domestic or irrigation use during the dry season.

5.2 Discussion of the methodology

One of the objectives was to use PEST to calibrate for ET. As this parameter was unknown in all computational period, the validation would only validate the other input parameters, however, at the same time compute the unknown ET. It is questionable how reliable the validation would have been, having an unknown parameter. Furthermore, relating ET to groundwater irrigation is assumption that was made. However, since the model did not take vegetation and characteristics of the unsaturated zone into account, and ET does not take into account the physical background of ET, it was possible to relate ET with irrigation in this case, using ET as a balancing variable balancing the computed and measured water table for a better fit.

5.3 Limitations of the model input parameters

The study showed several limitations including stratigraphy, recharge, and evapotranspiration parameter. Furthermore, the GMS MODFLOW software has its limitations.

Regarding the stratigraphy of the aquifer layers, this analysis was only based on the information provided by Michael Roberts giving layer elevations for young alluvium and old alluvium measured at the PRASAC wells. Thus, there were less than 50 measurements used for interpolating the surface to the model boundaries. Especially the part towards Vietnam was sparse in data, the same accounts for the water level measurements, which were not available for the part further south towards Vietnam. Furthermore, the deeper aquifer below the depth that PRASAC wells reach was highly unknown. Making assumptions on unknown bedrock elevations is generally difficult and time consuming, considering that the interpolation of layer elevations to the MODFLOW grid is another challenging task. In this study the bottom of the aquifer was assumed in accordance with the PRASAC stratigraphic logs and based on the study of Erban and Gorelick. However, there are other studies showing indices that the bedrock reaches much deeper depths than 100 m which was assumed the deepest in this model: Kogyo (2002) provides a map on the estimated bedrock, giving several bedrock elevation points (**Appendix 1:** Estimated bedrock depth from Kogyo, 2002.). Some of those points reach depths of about 400 m below

MSL. The JICA/Kogyo map was established by test well drilling and resistivity soundings using Wenner's electrode configuration (Kogyo, 2002). Also the breakpoints from North-South and East-West cross sections provided by the IDE (2009) show bedrock elevations reaching 200 m depth (**Appendix 2**, **Appendix 3**, **Appendix 4**). Hence, it shows that the bedrock depth is highly uncertain, and questions the reliability of the used data. For the purpose of this study, relating the irrigation practises to the groundwater storage, it was enough to assume the bottom aquifer elevations according to the stratigraphy of the PRASAC wells. It should be further studied if it makes a difference to use deeper bedrock elevations as were interpolated from IDE and JICA and shown in **Appendix 5**. More reliability could be added by investigating the deep aquifer. However, this will be a rather costly, effort rich and time-consuming investigation.

The field visit to Cambodia gave access to other necessary data such as the historical water level time series. Nonetheless, the water level time series suffer from data lacks which were interpolated by taking the average value for the same month for the preceding and subsequent year in order to receive a continuous dataset. Furthermore, looking through the dataset it was noticeable that four wells must have been confused with another well location for the years 2015 to 2022. Despite that the recent database seems to be developed and improved. It seems as if efforts are taken nowadays to take monthly measurements for the available wells, which is promising for future studies.

Though there are several rivers in the study area, the Mekong River was used as main source/sink and model boundary simultaneously. It would add detail to add smaller rivers to the model as well, though data on water heads was not available for these smaller rivers. The outflow section of the eastern boundary was based on literature (IDE, 2009) and seasonal variations were assumed to be neglectable. More detailed knowledge on this part of the boundary would add detail to the model boundary conditions.

The specification of the recharge zone in the northeast of the model was similar in IDE (2009) and Erban and Gorelick (2016) and done accordingly in this model. Also recharge rate were similar in those two studies and the recharge rate was based on those studies and also calibration outcomes. Other earlier studies, however, propose much higher recharge rates: Rasmussen (1977) assumed that the annual recharge to the aquifer by rainfall is about 150 mm,

where 100 mm can be “recoverable”. Kogyo (2002), estimated the recharge to be around 448 mm per year (34.1 % of rainfall), which is much higher than estimations by other studies, hence, likely to be overestimated. The NexView Frontier Groundwater Model 2020 used uniform recharge with about 16 % of precipitation, resulting in about 0.25 m per year, which is also much higher than what was assumed by IDE and Erban and Gorelick. Another aspect regarding recharge is simplification to monthly recharge values in the transient model which were generalised for each year. Thus, seasonal variations are accounted for, but not the variations between different years. This could be improved by basing the recharge values on precipitation pattern for each month in each year, thereby accounting for climatic changes.

Another question to add to discussion is why the recharge parameter was added to the steady state model, even though it determines vertical movement of water, and should, thus, theoretically not be included in the steady state model. However, it was impossible to receive a good calibration result without adding water into the system, besides the Mekong River source. Adding the recharge parameter is motivated by referring to the IDE (2009) study who also applied recharge to the steady state condition. It was done accordingly and with similar values in this study, though it still needs to be considered with caution, as ET and pumping were only added in the transient state model.

One of the important aspects was applying the Evapotranspiration package in GMS MODFLOW. ET rate was relatively easy to determine from ground surface elevation and calibration, respectively, but the extinction depth was more challenging to be determined. The theory was employed to set extinction depth according to the root depth of the prevailing vegetation, though the roots of rice are very shallow, only allowing a depth of maximum 50 cm to experience ET, since the model assumes ET only in between the ET surface and the ET extinction depth. In addition, making assumptions on the relationship of hydraulic head and ET rate was highly speculative and only based on the attempt to receive better calibration results. Gelsinari et al. (2020) uses an ET assimilation framework to assess a conceptual and a physically based model of the unsaturated zone which is being coupled to MODFLOW to improve the groundwater model output. Extensions of the MODFLLOW software like suggested by Gelsinari et al. (2020) could improve the uncertainties that accompanied the use of the ETS package. Though, this would be a comprehensive assessment and would perhaps contribute to a whole new

study itself. Furthermore, as touched beforehand, climate aspects were not considered in this study, but they are expected to have effect on both, groundwater level and ET. Neglecting the climate aspects was done to simplify this study. Improvement could be made by examining the effect of temperature, radiation and rainfall on the water level as well as the ET.

5.4 Evaluation of the software GMS MODFLOW

Nowadays, the software GMS MODFLOW is broadly adopted to find solutions to the groundwater flow equation. This software is using the finite difference method with realistic documented and also open source. Using the finite-difference helps users to understand easily and analyse subsurface conditions. The grid is simple and straight forward to implement, however, designing the grid in terms of resolution, has effects on the calculations and refinement of the groundwater model, thus, needs to be done with caution. Although GMS is user-friendly and easy to use, there are some disadvantages that cause uncertainty in results. One of the challenges in using GMS software is that there are several amounts of uncertainty related to a groundwater model that is highly simplified and conceptualized: Uncertainties in existing data, the conceptual model, and simplifications in entering parameters to the model such as recharge rate, hydraulic conductivity, specific yield or specific storage that can cause further uncertainty in the results. To mitigate this uncertainty, it is suggested to calibrate a model with observation data like different monitoring wells, flows of stream, etc. However, maintaining a well-calibrated model, and accounting for the uncertainty in the groundwater model and original assumptions of e.g., hydraulic conductivities or recharge, all at the same time, is challenging (Aquaveo, 2018). Another challenge in GMS is that complex geological characteristics such as angled faults and sharp hydraulic gradients cannot be modelled in this software (Kumar, 2019), but somehow be accounted for by adapting the input data. However, in the end GMS remains a powerful and user-friendly tool with big potential when having sufficient and reliable data.

6. Conclusion

This study investigated the relationship of irrigation changes and aquifer storage by creating a groundwater model (firstly steady state, then transient state) using GMS MODFLOW to relate irrigation changes with changes in groundwater level, by assuming evapotranspiration (ET) is an indicator of groundwater irrigation. The study area was south-eastern Cambodia, where groundwater is extensively used for rice irrigation during the dry season, causing water levels to fall below a pumping limit (6 m). The focus was put on the provinces Prey Veng and Svay Rieng, where observation wells are installed providing necessary groundwater level data for a groundwater model.

The objective to collect data (groundwater level and information on geology) on a field visit to Prey Veng and Svay Rieng was successfully achieved. With the data, a steady state groundwater model for the study area could be established, which was the second objective. The third objective was to create a transient model. It was possible to do a sensitivity analysis for the steady state model, and calibrate recharge, specific storage and specific yield, however, it was not possible to apply automated parameter estimation of ET using the PEST algorithm. This was due to high computational effort of the algorithm, and high error occurrence when applying PEST, being unable to perform a successful run. Thus, ET estimates could not be produced for the pre- pandemic and pandemic time and outcomes were not compared to the remote sensing outcomes, which was the immediate aim of this study. Looking at the collected groundwater level data, an increased decline in most of the wells water level was seen in the pandemic time, resulting in many wells having water levels below 6 m depth, which is not sufficient for pumping anymore. This suggests that there was an overall increase in agricultural activity during the pandemic time, which is the opposite from what was suggested by the NDVI remote sensing analysis. However, climatic changes or increased usage of water in households are other factors besides higher irrigation increase that could have affected the decline in groundwater level. Immediate action to develop measures to control groundwater extraction are strongly recommended to be taken.

The discussion showed the high deviations of recharge parameter and bedrock elevation, between the different other studies. However, Erban and Gorelick, and IDE`s study generally showed a rather similar approach and thus, this study used their approaches in a combined way to receive sufficient input to

the model. Since various model parameters were showing different values in different studies, the reliability can be set in question and having more reliable measurements on those parameters should be further investigated for future groundwater studies in Prey Veng and Svay Rieng. For the purpose of this study, relating the irrigation practises to the groundwater storage, the available data was considered to be sufficient, despite uncertainties, however the model may have been too complicated for the automated parameter estimation to be successful.

References

- Aquaveo, 2022. GMS: ETS Package [Online]. Available: https://www.xmswiki.com/wiki/GMS:ETS_Package [Accessed 01.06.2022].
- Asian Development Bank (ADB), 2019. Characterizing water supply and demand in Cambodia's river basins. Available: Characterizing Water Supply and Demand in Cambodia's River Basins (adb.org) [Accessed 12.05.2022].
- Barua, K. 2020. Supporting Cambodian farmers during the COVID-19 pandemic [Online]. IFAD. Available: https://beta.ifad.org/en/web/latest/-/blog/supporting-cambodian-farmers-during-the-covid-19-pandemic [Accessed 06.10.2021].
- Camboja News. 2017. Overview of 2016 Natural Disasters. ClimaTemps. 2021. Phnom Penh Climate & Temperature [Online]. Available: http://www.phnompenh.climatemps.com/ [Accessed].
- Ceicdata.com. 2022. Cambodia Population: Census: Prey Veng/Svay Rieng [Online]. Available: https://www.ceicdata.com [Accessed 01.06.2022].
- Erban, L. E. & Gorelick, S. M. 2016. Closing the irrigation deficit in Cambodia: Implications for transboundary impacts on groundwater and Mekong River flow. Journal of Hydrology, 535, 85-92.
- Esri, 2012. Empirical Bayesian Kriging. Empirical Bayesian Kriging (esri.com). [Accessed 01.05.2022].
- Esri, 2020. ArcGIS Desktop. Available: ArcGIS Desktop | Desktop GIS Software Suite (esri.com)
- FAU College of Engineering, 2022. Extinction depth. Available: https://www.cse.fau.edu/~maria/ed.html [Accessed 15.06.2022].
- Fetter, C.W. (2001). Applied Hydrogeology. Fourth Edition.
- Gelsinari, S., Pauwels, V., Daly, E., Dam, J. C., Uijlenhoet, R. & Doble, R. 2020. Unsaturated zone model complexity for the assimilation of evapotranspiration rates in groundwater modeling.
- Hashemi, H., Berndtsson, R., Kompanizare, M. & Persson, M. 2012. Natural vs. artificial groundwater recharge, quantification through inverse modeling. Hydrology and Earth System Sciences, 9, 9767-9807. Available: https://hess.copernicus.org/articles/17/637/2013/hess-17-637-2013.pdf [Accessed 03.06.2022].
- International Development Enterprises Cambodia (IDE). 2005. National Committee for sub-national democratic developement rural poverty reduction project. Strategic study of groundwater resources in Prey Veng and Svay Rieng (Phase 1).
- IFC, 2015 Cambodia Rice- Export Potential and Strategies. Available: https://openknowledge.worldbank.org/bitstream/handle/10986/26109/111938-WP-Cambodia-Market-Survey-Final-2015-PUBLIC.pdf?sequence=1&isAllowed=y [Accessed 03.05.2022].
- International Development Enterprises Cambodia (IDE). 2009. National Committee for sub-national democratic developement rural poverty reduction project. Strategic study of groundwater resources in Prey Veng and Svay Rieng (Phase 2).
- Keng, B. & Rim, S. 2021 The Impact of COVID-19 on Cambodian Farmers [Online]. CambodianessThmeyThmey in English. Available: https://cambodianess.com/article/the-impact-of-covid-19-oncambodian-farmers [Accessed 13.10.2021]
- Kogyu, K. (2002). The Study on Groundwater Development in Southern Cambodia.
- Medium. 2016. MAE and RMSE — Which Metric is Better? [Online]. Available: https://medium.com/human-in-a-machine-world/mae-and-rmse-which-metric-is-better-e60ac3bde13d [Accessed 12.05.2022].
- Mekong River Commission (MRC), 2022. MRC time-series inventory. Available: MRC - Data Portal (mrcmekong.org) [Accessed 29.04.2022].
- Misachi, J. 2021. Mekong River [Online]. WorldAtlas. [Accessed]. Modis Resolution Imaging Spectroradiometer (MODIS). 2021. MODIS Vegetation Index Products (NDVI and EVI) [Online]. Available: https://modis.gsfc.nasa.gov/data/dataprod/mod13.php [Accessed 31.10.2021].
- Oeurng, C. 2020 Development of Groundwater Management Strategy in Cambodia.
- Rasmussen, W.C., and Bradford, G.M., 1977: Ground-Water Resources of Cambodia, Water-Supply Paper 1608-P, United States Geological Survey, Washington DC.
- Roberts, M.S., 1998: Groundwater Irrigation in the Mekong Delta of Cambodia, M.Sc Thesis, Cornell University, Ithaca, New York.

- Statistics How To, 2016. Mean Error: Definition [Online]. Available: https://www.statisticshowto.com/mean-error/ [Accessed 15.05.2022].
- The Phnom Penh Post. 2021. Cambodian farmers hit hard by Covid-19 pandemic, NGOs find.
- UNDP Cambodia. 2020. Living in Rural Cambodia during COVID-19: Examples from Farming Communities.
- USGS, 2020. NexView Frontier Groundwater Model, Available: D2_3_Kyle Davis.pdf

Appendix

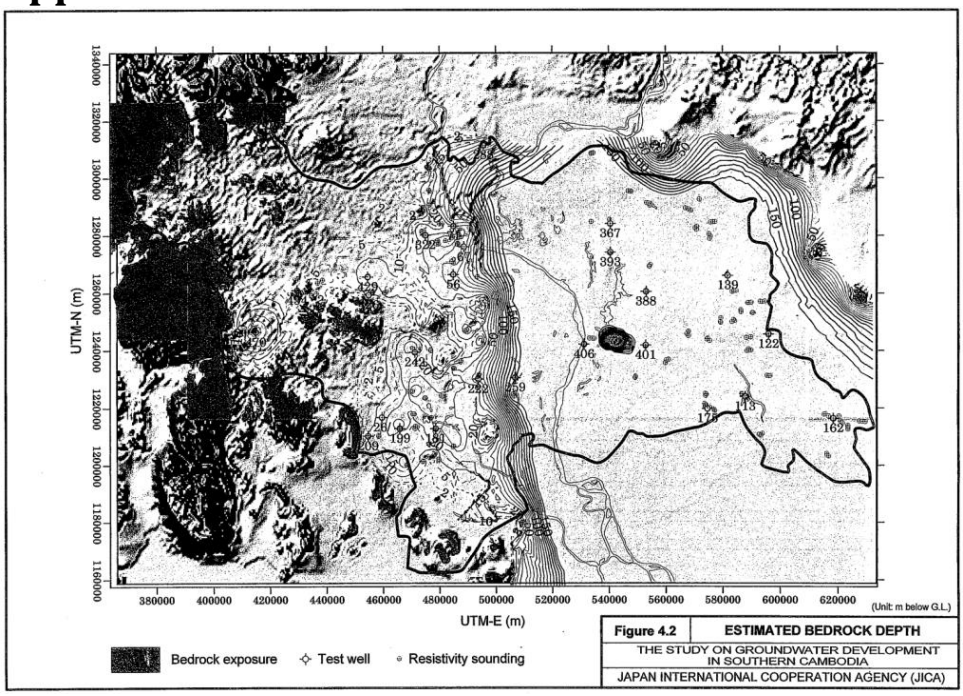

Appendix 1: *Estimated bedrock depth from Kogyo, 2002.*

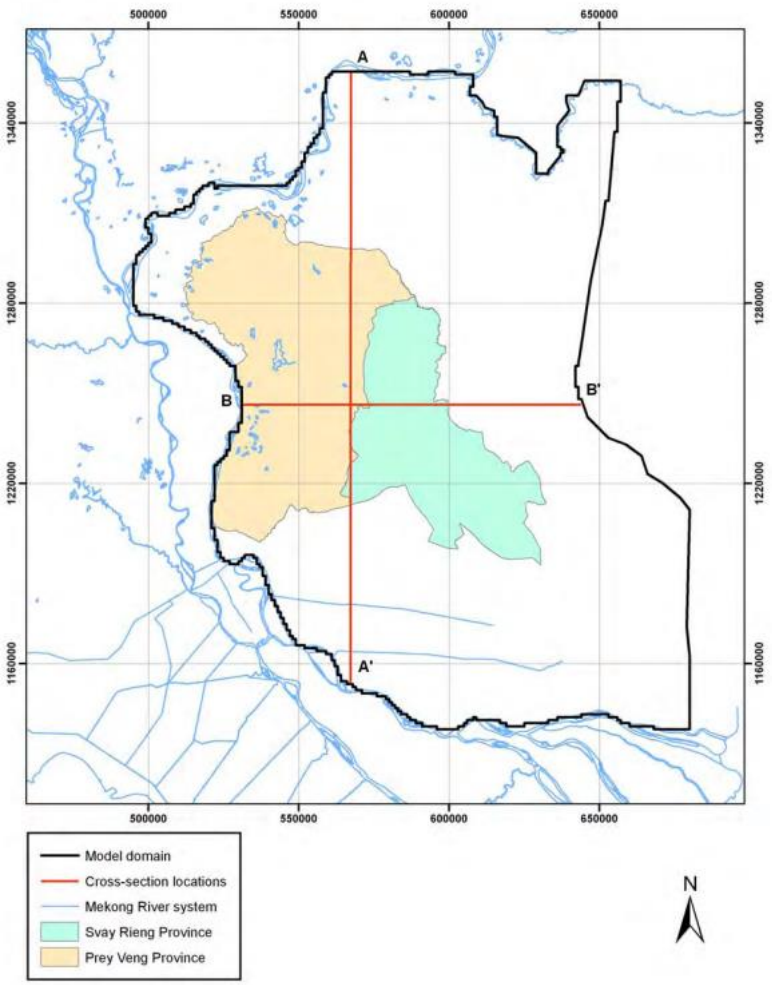

Appendix 2: *Figure of the cross sections A-A' (north to south) and B-B' (west to east) (Source: IDE, 2009).*

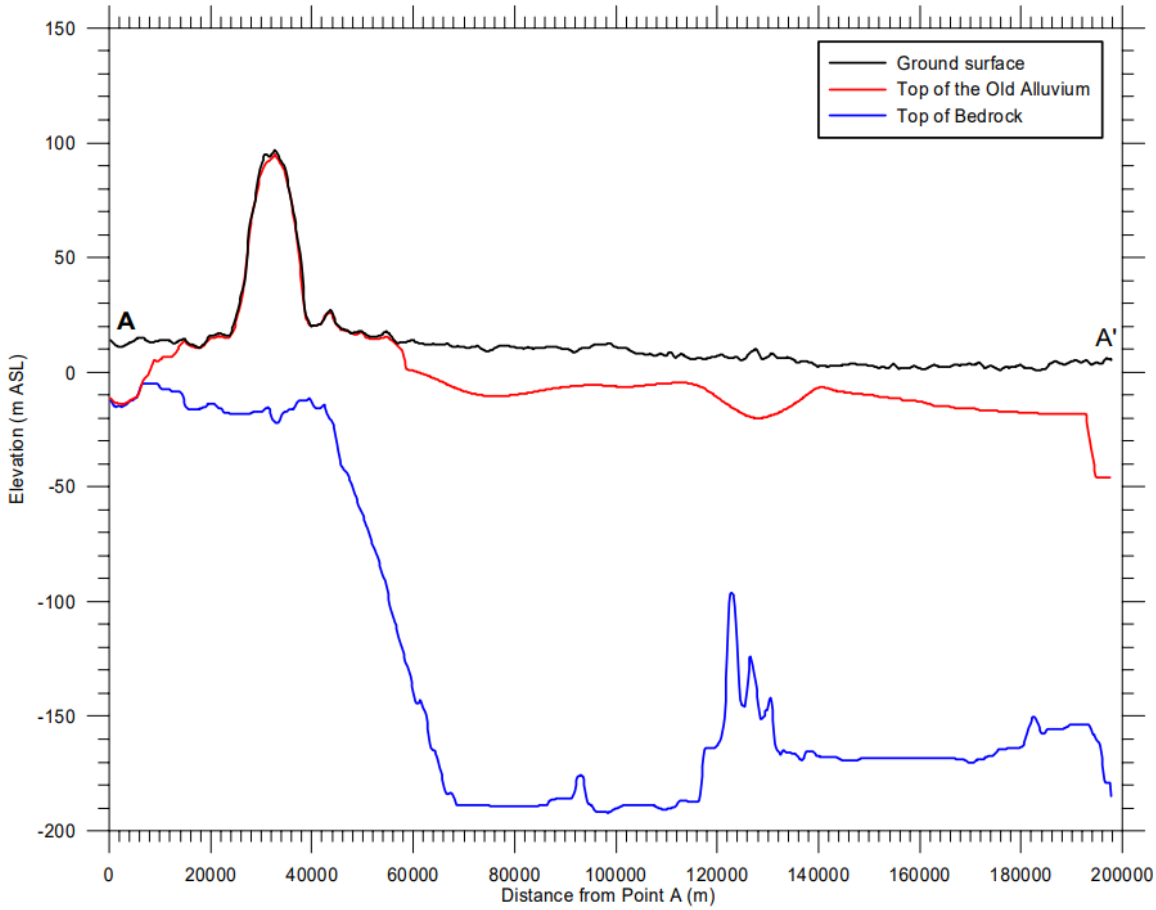

Appendix 3: *North to south cross section (A to A') (Source: IDE, 2009).*

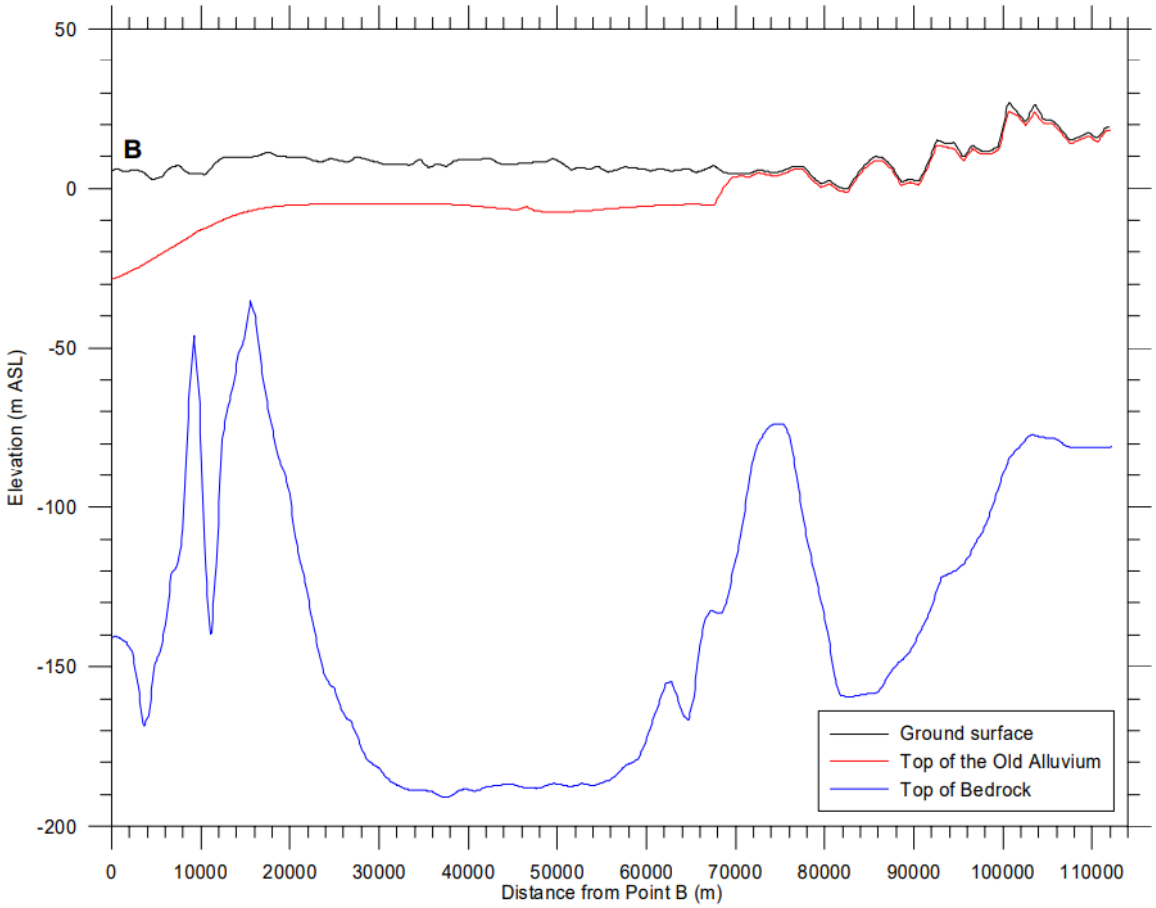

Appendix 4: *West to east cross section (B to B') (Source: IDE, 2009).*

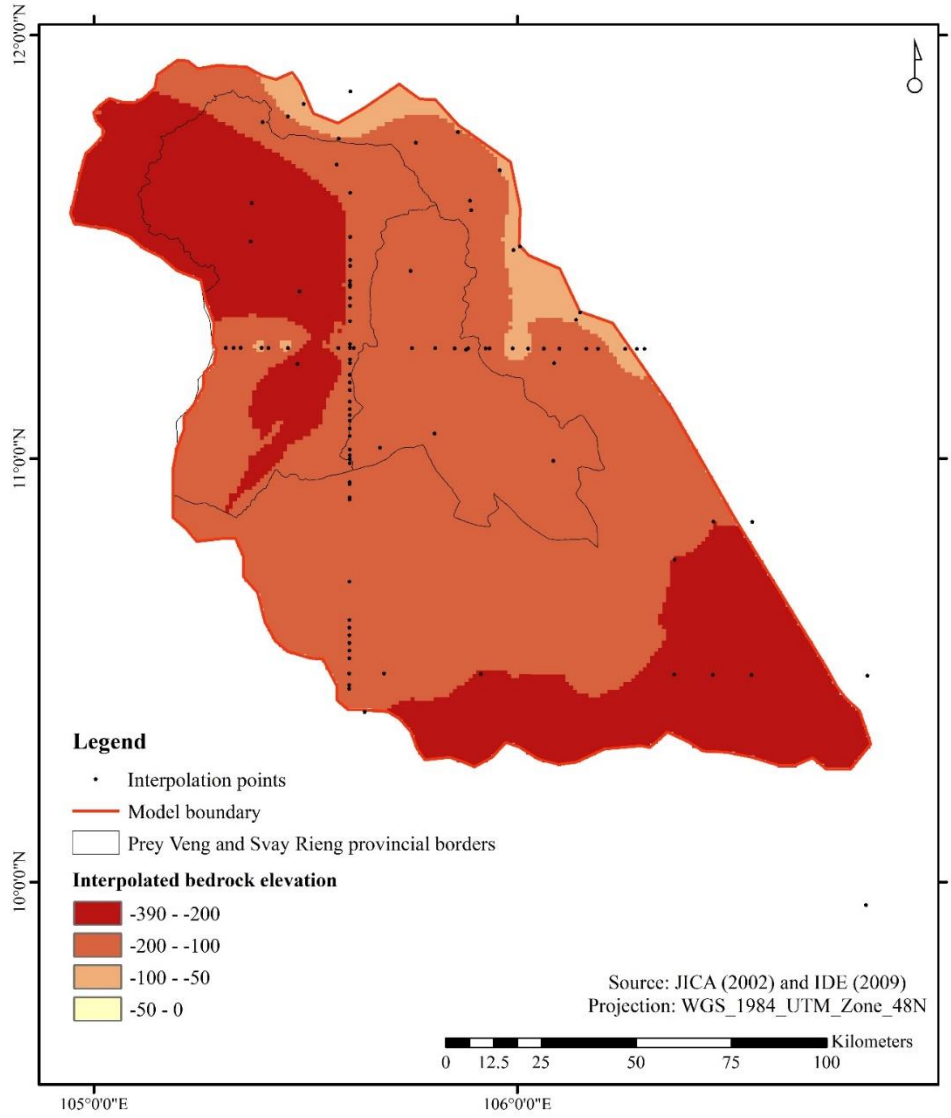

Appendix 5: *Alternative to the bedrock surface/ aquifer bottom used in this study.*

NO	DISTRICT	DATEDRILLE	TOTALDEPTH	SCREEN	X	Y	ALTITUDE
P1	Kompong Liew	1/31/1996	42.23	38	536900	1269900	8
P3	Prey Veng	02/05/1996	39.23	34	546200	1279100	10.2
P4	Prey Veng	02/05/1996	30	24	556600	1282300	10
P5	Prey Veng	2/13/1996	48	44	558800	1268300	7.2
P6	Kamchay Mear	2/13/1996	40.73	36.6	573800	1272400	10.5
P7	Kamchay Mear	2/15/1996	36	32	572700	1279800	6
P8	Kamchay Mear	03/12/1996	101.3	81	574600	1285000	8.3
P9	Kanh Chreach	3/19/1996	36.23	32	578800	1295500	14
P10	Kanh Chreach	3/22/1996	34.73	30.5	556500	1288300	11.2
P11	Sithor Kanda	3/21/1996	43.5	38	543500	1308400	10.5
P12	Sithor Kanda	3/24/1996	34.5	29	533700	1308100	10
P13	Peareang	3/15/1996	34.73	30	518200	1299800	9.6
P14	Peareang	3/17/1996	39.73	35.5	514200	1290000	10.5
P15	Peareang	03/05/1996	79.6	57.8	525900	1285700	8.8
P16	Kampong Liew	3/14/1996	56	50	525000	1269900	4
P17	Peam Ro	03/12/1996	48.23	44.4	529500	1256800	5.5
P18	Ba Phnom	2/26/1996	46.5	42.5	543700	1257000	8
P19	Ba Phnom	2/23/1996	37.5	33.5	545800	1237900	6
P20	Mesang	03/06/1996	101.3	26.3	559700	1256300	6.3
P21	Mesang	2/14/1996	35	31	571000	1254500	7
P22	Kpg Trabek	2/18/1996	37	33	563000	1236000	7
P23	Kpg Trabek	2/21/1996	46.73	42.5	561000	1229000	5.5
P24	Kpg Trabek	2/22/1996	48	44	567300	1230200	5.5
P25	Kpg Trabek	2/23/1996	48.23	44	557800	1215200	4
P26	Preah Sdach	2/27/1996	40.73	36	544500	1225600	4.8
P27	Preah Sdach	03/03/1996	101.3	79.5	544500	1224500	4.3
P28	Peam Chor	03/01/1996	48.27	37.73	530100	1239000	5.8
P29	Peam Chor	03/02/1996	44	40	523800	1222200	5.3
P30	Peam Chor	03/10/1996	55.5	50	522300	1207000	4
P31	Peam Chor	03/08/1996	51.23	28.5	536600	1206000	2.4
S1	Svay Chrum	03/01/1996	88.9	65	581000	1222700	3.9
S2	Svay Chrum	03/11/1996	37	29	566000	1216800	3.2
S3	Svay Chrum	3/15/1996	34.5	30.5	571400	1241300	6
S4	Svay Chrum	2/14/1996	45	37.5	579700	1229800	4.8
S5	Romeas Hek	5/17/1996	22	18	578900	1263000	7
S6	Romeas Hek	2/26/1996	36	31.5	584200	1255700	5
S7	Romeas Hek	5/15/1996	29	24	587900	1265000	7
S8	Romeas Hek	2/29/1996	33	26.5	595800	1253000	5
S9	Romdoul	2/21/1996	40.5	37	581800	1242300	7.3
S10	Romdoul	2/28/1996	33	29	598400	1242800	7.5
S11	Svay Teap	2/19/1996	39	33	597200	1232200	5.8
S12	Svay Teap	03/01/1996	36	30.5	601000	1232800	6
S13	Svay Teap	03/05/1996	39	35	614900	1225500	4.7
S14	Chantrea	2/27/1996	96.6	42	627100	1223500	3.7
S15	Chantrea	03/02/1996	33	22.5	623900	1209100	2
S16	Chantrea	03/05/1996	39	29	625212	1198937	1.3
S17	Kompong Ro	03/06/1996	28.5	21	603800	1217800	4.5
S18	Kompong Ro	03/07/1996	34.5	30.5	606400	1205500	3.3
S19	Kompong Ro	3/14/1996	47	36.5	594500	1213000	3.8

Appendix 6: *Details on installation, location, depths and elevation of the PRASAC observation wells.*

Name	Code	Country	Parameter	Type	Unit	River	Interval	Data Start*	Data End*
Chroy Chang Var	19801	Cambodia	Water Level	Manual	m	Mekong	1-6 times p/day	19600101	20121231
Kompong Cham	19802	Cambodia	Water Level	Manual	m	Mekong	1-6 times p/day	19300101	20220502
Neak Luong	19806	Cambodia	Water Level	Manual	m	Mekong	1-6 times p/day	19260101	20220502
My Thuan	19804	Viet Nam	Water Level	Manual	m	Mekong	1-6 times p/day	19600630	20220502
Vam Kenh	985203	Viet Nam	Water Level	Manual	m	Mekong	1-6 times p/day	19920101	20220502
Tan Chau	19803	Viet Nam	Water Level	Manual	m	Mekong	1-6 times p/day	19790401	20220502

Appendix 7: *Details on the gauge station measuring the daily water levels of the Mekong River.*